Geometry of Integers

Hassan BALOUI

hassan.baloui@gmail.com

DOI: 10.5281/zenodo.23456718

Abstract

On the classical one-dimensional number line, the structural depth of an integer—its step distance from the origin—coincides identically with its scalar magnitude. Confined to a single degree of freedom, integers can translate only forward or backward along a single flat axis. This paper constructs an infinite hierarchy of higher-degree discrete integer foliations and their reflected integer completions, within which the longitudinal depth of an integer along its structural leaves is decoupled from its ambient scalar magnitude. By partitioning the integers into horizontal power shells aligned along a central median spine, every integer generates its own intrinsic two-dimensional coordinates across three canonical directional directions. This foliated architecture induces a direction-dependent discrete transport operator that simultaneously generates a global Chebyshev geodesic metric and a native multi-valued, non-commutative, and non-distributive arithmetic governing foliated addition, subtraction, multiplication, division, and primality. Furthermore, whereas global scalar primes scatter across shells, local leaf-depth primality endows every individual leaf with an autonomous Fundamental Theorem of Arithmetic, assigning each integer a coupled triad of unique prime factorizations. In the quadratic foliation, magnitude-coupled self-shift transport exhibits non-vanishing discrete holonomy, positive discrete curvature that converges asymptotically to a constant under quadratic normalization, and an exact holographic conservation law linking prime counts in the initial interval to the corresponding quadratic shell. Finally, under the correspondence principle at degree one, the lateral generators, discrete holonomy, and curvature vanish identically; the integers lose their second degree of freedom, and classical commutative Peano arithmetic is restored on the one-dimensional number line.

Contents

1 Introduction **3**

2 Foliation of Integers **5**

2.1 The Quadratic Foliation ($m = 2$) 5

2.1.1 Geometry and the Four Intrinsic Partitions 5

2.1.2 Intrinsic Coordinate Extraction and the Transport Operator ∇_λ 7

2.1.3 1-Zigzag Geodesic Routing and the Chebyshev Metric on $\mathbb{N}_2$ 8

2.2 The m-Degree Foliation ($m > 2$) 9

2.2.1 Power Shells, Medians, and Leaf Parameterizations 9

2.2.2 Coordinate Extraction, Global Transport, and the Chebyshev Metric in $\mathbb{N}_m$ 10

3 Foliated Arithmetic **12**

3.1 Foliated Addition and Multiplication in $\mathbb{N}_2$ and $\mathbb{N}_m$ 12

3.1.1 Cross-Direction Intersections in $\mathbb{N}_2$ vs. Absolute Disjointness for $m \geq 3$. 12

3.1.2 Non-Distributivity of Foliated Arithmetic 14

3.2 The Reflected Double-Lattice $\mathbb{Z}_m$: Subtraction and Four-Quadrant Multiplication 14

3.2.1 Four-Quadrant Foliated Addition, Subtraction, and Multiplication 15

3.2.2 Foliated Exponentiation: Leaf-Conserving and Left-Recursive Powers . . . 18

3.3 Foliated Euclidean Division and Modular Arithmetic . . . 19
3.4 Direction-Dependent Foliated Primality . . . 20
3.4.1 Global λ-Foliated Primality (Irreducibility Under $\otimes_{\lambda,m}$) . . . 21
3.4.2 Local Leaf-Depth Primality and Intrinsic Leaf Classification . . . 21
3.4.3 Leaf-Local Fundamental Theorem of Arithmetic and Triadic Coupling . . . 22

4 Discrete Holonomy and Arithmetic Holography in $\mathbb{N}_2$ 24
4.1 Shell-to-Leaf Holographic Encoding . . . 24
4.2 Discrete Holonomy and Curvature on $\mathbb{N}_2$ and $\mathbb{Z}_2$ . . . 26
4.3 Conical Embedding of the Quadratic Foliation $\mathbb{Z}_2$ . . . 28
4.4 The Arithmetic Holographic Conjecture: Prime Packets and Sieve Coupling . . . 28
4.4.1 From Pointwise Prime Gaps to Shell Prime Packets . . . 28
4.4.2 Exact Holographic Conservation of Local Prime-Depth Elements . . . 29
4.4.3 The Arithmetic Holographic Conjecture and the $m = 2$ Riemann Hypothesis Bound . . . 30

5 The Correspondence Principle: Peano Arithmetic ($m = 1$) 31
5.1 Coordinate Degeneracy to the 1D Euclidean Line . . . 31
5.2 Degeneracy of Transport, Arithmetic, Division, Primality, Holonomy, and Metric 31

6 Discussion and Conclusion 32
6.1 Synthesis of the Foliated Arithmetic Framework . . . 32
6.2 Structural Parallels with Theoretical Physics and Computation . . . 33
6.3 Beyond the Integers: Open Questions for Algebra and the Continuum . . . 33

1 Introduction

At the foundational level of elementary arithmetic, the natural numbers $\mathbb{N} = \{0, 1, 2, \dots\}$ (with $\mathbb{N}^* = \mathbb{N} \setminus \{0\}$) and the ring of integers $\mathbb{Z}$ are universally constructed as one-dimensional scalars residing on a flat, featureless line. From the Euclidean and Cartesian traditions [1] to the axiomatizations of Dedekind and Peano [2, 3], standard arithmetic models the integers as a single linear sequence generated by a uniform successor step. Confined to a single degree of freedom, an integer's structural depth from the origin coincides identically with its scalar magnitude, restricting translation to commuting forward or backward shifts along a single axis. Consequently, within classical Peano arithmetic, the underlying set of integers possesses no intrinsic multi-dimensional geometry: numbers occupy dimensionless points on a flat line, while addition and multiplication operate as purely scalar algebraic rules devoid of transverse directions or internal curvature. As Tim Maudlin observed in *New Foundations for Physical Geometry* [4], classical arithmetic operations—particularly multiplication—possess no natural geometric realization on a one-dimensional linear structure.

Extrinsic versus Intrinsic Geometries of Numbers

Whenever classical mathematics has sought to endow the integers with geometric structure, it has treated the integers themselves as geometrically flat, importing distance, volume, or curvature from an external continuous space. Historically, efforts to bridge number theory and geometry have followed four main paradigms:

1. **The Peano–Dedekind Linear Paradigm:** Under the Peano axioms [3, 2], $\mathbb{Z}$ is formulated as a one-dimensional ordered ring. Because scalar magnitude and coordinate depth coincide, all directional translations commute, lateral width is zero, and the structure possesses no intrinsic curvature.

2. **Minkowski's *Geometrie der Zahlen*:** Hermann Minkowski's *Geometry of Numbers* [5] established that continuous spatial properties, such as convex bodies and volumes, govern the existence of discrete integer solutions. Yet Minkowski embedded $\mathbb{Z}^n$ as a static Cartesian grid inside the continuous Euclidean space $\mathbb{R}^n$. In Minkowski's architecture, all metric concepts—distance, volume, and convexity—belong to the ambient real continuum, while the integers remain a passive grid exerting no influence upon the space.

3. **Grothendieck's Arithmetic Schemes ($\mathrm{Spec}(\mathbb{Z})$):** In the 1960s, A. Grothendieck recast commutative rings as topological schemes [6], viewing $\mathrm{Spec}(\mathbb{Z})$ as a one-dimensional topological curve whose points correspond to prime ideals. However, $\mathrm{Spec}(\mathbb{Z})$ is an abstract Zariski-topological object lacking an intrinsic distance metric or discrete curvature.

4. **Arakelov Geometry:** In the 1970s, Suren Arakelov compactified $\mathrm{Spec}(\mathbb{Z})$ by adjoining "Archimedean fibers at infinity" [7], embedding the integers into the complex plane $\mathbb{C}$ and equipping the infinite fiber with continuous Hermitian metrics. Once again, the resulting curvature is imported extrinsically from the continuous complex plane rather than generated by the discrete integers themselves.

In contrast to this tradition, the present work constructs a purely *intrinsic* discrete geometry of the integers without embedding them into an external Euclidean space $\mathbb{R}^n$ or importing continuous metrics from $\mathbb{C}$. We demonstrate that when the integers are partitioned into their natural m-th power intervals, a metrizable, curved discrete geometry is already native to the integers themselves.

Epistemological Remark: Breaking the One-Dimensional Axiom of the Integers

For over two millennia, from Euclid and Diophantus to modern analytic number theory, mathematics has operated under an unstated ontological axiom: that the rational integers $\mathbb{Z}$ are intrinsically *one-dimensional*, each integer confined to a single degree of freedom along a flat line where longitudinal depth from the origin, scalar magnitude, and multiplicative identity are one and the same. Even when modern number theory embeds $\mathbb{Z}$ into higher-dimensional algebraic number rings, p-adic completions, or arithmetic schemes, the underlying rational integer itself remains locked to the flat one-dimensional Peano line ($m = 1$), devoid of lateral width or transverse directions.

The foundational shift of the *Geometry of Integers* is to recognize that this one-dimensional confinement is merely a degenerate flat limit. By lifting $\mathbb{N}$ and $\mathbb{Z}$ into an m-degree discrete foliation ($m \geq 2$), we grant the integers a second, intrinsic transverse degree of freedom along two complementary axes: we *decouple* scalar magnitude from longitudinal leaf depth—unfolding each integer into a two-dimensional coordinate triad equipped with simultaneous leaf-local prime factorizations—while directly *coupling* the global geodesic metric to the discrete transport operator.

The Architecture of Integer Foliations and Foliated Arithmetic

In this paper, we grant the integers a second degree of freedom within a two-dimensional discrete lattice through the construction of *Foliations of Integers* ($\mathbb{N}_m$ and their reflected completions $\mathbb{Z}_m$). For any fixed degree $m \geq 2$, we partition the natural numbers into horizontal intervals—termed shells—between consecutive m-th powers, $S_{k,m} = \{k^m, k^m+1, \ldots, (k+1)^m-1\}$. Because consecutive m-th powers always have opposite parities, every shell has odd cardinality and possesses a unique integer median:

$$V_{0,m}(k) = \frac{(k+1)^m + k^m - 1}{2}, \qquad k \in \mathbb{N}.$$

Aligning these medians along a central vertical spine causes the remaining integers to self-organize laterally across each shell. An interior integer thereby transitions from having only two neighbors on a one-dimensional line (one predecessor and one successor) to inhabiting a two-dimensional neighborhood across adjacent shells and transverse trajectories—termed *leaves*—that originate at boundary roots possessing no predecessors along their respective directions.

Within each m-foliation, longitudinal depth along a leaf is decoupled from scalar magnitude. Every integer is simultaneously indexed by a lateral generator (identifying its resident leaf) and a local longitudinal depth (measuring its step distance from that leaf's birth shell) across three canonical directions: left-curved, vertical, and right-curved. While shell cardinalities grow as polynomials of degree $m - 1$, the scalar magnitudes form bijective polynomials of degree m in the local coordinates [8, 9]. The integers thus function both as scalar magnitudes and as two-dimensional lattice coordinates, endowing each foliation $\mathbb{N}_m$ with a global geodesic distance equivalent to the Chebyshev (L^∞) metric.

Passing from the flat line ($m = 1$) to higher-degree foliations ($m \geq 2$) fundamentally transforms arithmetic. On the one-dimensional line, commutativity guarantees path independence. In a foliated lattice, longitudinal transport along the three canonical leaf directions is governed by a direction-dependent shift operator. Because horizontal shells widen polynomially with depth while lateral generators remain constant along leaves, sequential translations along distinct directions fail to commute, and binary arithmetic operations—addition, subtraction, multiplication, and Euclidean division—map pairs of integers to multi-valued directional triads rather than single scalars.

At the same time, this decoupling resolves the classical tension between additive translation and multiplicative primality. Whereas global scalar primes scatter irregularly across shells,

measuring divisibility by intrinsic leaf depth endows every individual leaf with an autonomous copy of the Fundamental Theorem of Arithmetic. Because every integer sits at the transverse intersection of three directional leaves, each integer carries three simultaneous, rigidly coupled canonical prime factorizations—which in the quadratic foliation ($m = 2$) directly link boundary leaf-depth primes to Goldbach partitions of the shell index.

Following the geometric construction of the m-degree integer foliations and their geodesic metric (Section 2), we formulate multi-valued foliated arithmetic, Euclidean division, and the Leaf-Local Fundamental Theorem of Arithmetic on $\mathbb{N}_m$ and $\mathbb{Z}_m$ (Section 3). We then establish discrete holonomy, asymptotic curvature, and prime holography in the quadratic foliation (Section 4), prove the $m = 1$ Peano correspondence principle (Section 5), and examine implications for theoretical physics and higher-dimensional number systems (Section 6).

2 Foliation of Integers

2.1 The Quadratic Foliation ($m = 2$)

2.1.1 Geometry and the Four Intrinsic Partitions

For any non-negative integer $k \in \mathbb{N}$, consider the finite integer interval $S_k = \{k^2, k^2+1, \ldots, k^2+2k\}$. This interval has odd cardinality $|S_k| = 2k+1$ and a unique median located at the pronic number k^2+k. Every integer $n \in S_k$ therefore admits a symmetric reflection across this median given by $2(k^2+k) - n$.

By arranging these intervals horizontally on a two-dimensional discrete grid and aligning the medians $k^2 + k$ along a central vertical column, each interval S_k forms a horizontal shell at shell index k. Because the cardinality increases by exactly two elements per vertical step ($|S_{k+1}| - |S_k| = 2$), the outer boundaries—defined by the perfect squares k^2 on the left and their reflections $(k+1)^2 - 1$ on the right—form straight diagonal rays. The set $\mathbb{N}$ is thereby organized into a two-dimensional triangular lattice $\mathbb{N}_2$, governed globally by the reflection involution (Subfigure 1a):

$$\sigma_2(n) = 2\left(\lfloor\sqrt{n}\rfloor^2 + \lfloor\sqrt{n}\rfloor\right) - n. \tag{2.1}$$

While the horizontal shells $\{S_k\}_{k\in\mathbb{N}}$ form one disjoint partition of $\mathbb{N}$, three additional disjoint partitions into infinite one-dimensional trajectories—termed *leaves*—arise naturally on the lattice:

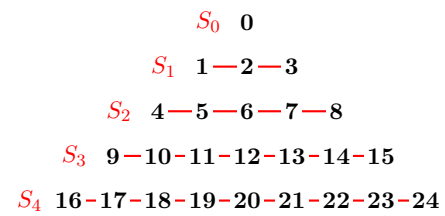
1. **The Vertical Frame (V_g, Subfigure 1b):** Drawing vertical columns downward from the boundary elements of each shell S_k parallel to the central pronic axis $V_0 = \{k^2+k\}_{k\in\mathbb{N}}$ partitions $\mathbb{N}_2$ into vertical leaves V_g indexed by $g \in \mathbb{Z}$ ($g > 0$ to the right of V_0, $g < 0$ to the left), satisfying:
$$\sigma_2(V_g) = V_{-g}, \qquad \sigma_2(V_{-g}) = V_g. \tag{2.2}$$

2. **The Left Diagonal Frame (L_g, Subfigure 1d):** Descending parallel to the left boundary ray of squares $L_0 = \{k^2\}_{k\in\mathbb{N}}$, the leaves L_1 and L_2 originate at $2, 3 \in S_1$, exhausting S_1, while subsequent leaves L_{2k-1}, L_{2k} originate at the two rightmost unassigned elements of each shell S_k.

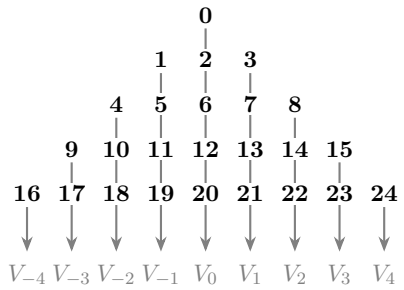
3. **The Right Diagonal Frame (R_g, Subfigure 1c):** Applying the reflection involution $\sigma_2(L_g) = R_g$ produces the right diagonal leaves descending parallel to $R_0 = \{k^2+2k\}_{k\in\mathbb{N}}$.

We derive the explicit polynomial parameterizations for each family of leaves in terms of the leaf **Generator** g and local **Depth** $d \in \mathbb{N}$:

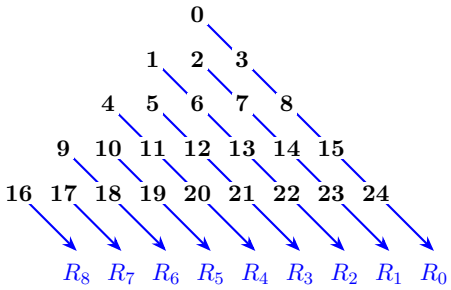
- **Horizontal Shell Coordinates (Figure 1a):** Any $n \in \mathbb{N}$ decomposes uniquely as $n = k^2 + r_n$, where $k = \lfloor\sqrt{n}\rfloor$ is the shell index and $0 \le r_n \le 2k$ is the intra-shell residue.



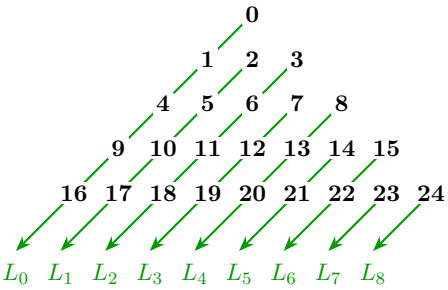
(a) The Horizontal Frame (S_k)



(b) The Vertical Frame (V_g)



(c) The Right Diagonal Frame (R_g)



(d) The Left Diagonal Frame (L_g)

Figure 1: The four intrinsic coordinate partitions of the quadratic foliation $\mathbb{N}_2$ for integers $0 \le n \le 24$.

- **Left and Right Vertical Leaves V_g (Figure 1b):** For $g > 0$, $V_{-g} = \{k^2+k-g \mid k \ge g\}$. Setting $d = k - g \in \mathbb{N}$ gives:

$$V_{-g} = \left\{(g+d)^2 + d \;\middle|\; d \in \mathbb{N}\right\}. \tag{2.3}$$

  Reflecting across V_0 gives $V_g = \sigma_2(V_{-g}) = \{(g+d)^2 + d + 2g \mid d \in \mathbb{N}\}$, which combines into a single equation for all $g \in \mathbb{Z}$:

$$V_g = \left\{(|g|+d)^2 + d + g + |g| \;\middle|\; (g,d) \in \mathbb{Z} \times \mathbb{N}\right\}. \tag{2.4}$$

- **Right Diagonal Leaves R_g (Figure 1c):** Even-indexed leaves $R_{2g} = \{k^2 + 2k - 2g \mid k \ge g\}$ $(d = k - g \in \mathbb{N})$ and odd-indexed leaves $R_{2g+1} = \{k^2 + 2k - (2g+1) \mid k \ge g+1\}$ $(d = k - g - 1 \in \mathbb{N})$ satisfy:

$$R_{2g} = \left\{(g+d)^2 + 2d \;\middle|\; d \in \mathbb{N}\right\}, \qquad R_{2g+1} = \left\{(g+d+1)^2 + 2(d+1) - 1 \;\middle|\; d \in \mathbb{N}\right\}, \tag{2.5}$$

  which consolidate for any $g \in \mathbb{N}$ (with birth shell $k_0 = \lceil g/2 \rceil$) into:

$$R_g = \left\{\left(\left\lceil \frac{g}{2} \right\rceil + d + 1\right)^2 - 1 - g \;\middle|\; d \in \mathbb{N}\right\}. \tag{2.6}$$

- **Left Diagonal Leaves L_g (Figure 1d):** Applying $\sigma_2(R_g) = L_g$ yields the even and odd branches:

$$L_{2g} = \left\{(g+d)^2 + 2g \;\middle|\; d \in \mathbb{N}\right\}, \qquad L_{2g+1} = \left\{(g+d+1)^2 + 2g + 1 \;\middle|\; d \in \mathbb{N}\right\}, \tag{2.7}$$

  which consolidate for any $g \in \mathbb{N}$ (with birth shell $k_0 = \lceil g/2 \rceil$) into:

$$L_g = \left\{\left(\left\lceil \frac{g}{2} \right\rceil + d\right)^2 + g \;\middle|\; d \in \mathbb{N}\right\}. \tag{2.8}$$

Because each of the four families $\{S_k\}$, $\{V_g\}$, $\{R_g\}$, and $\{L_g\}$ is a pairwise disjoint partition of $\mathbb{N}$, every integer $n \in \mathbb{N}_2$ is uniquely determined as the four-way intersection of one trajectory from each family:

$$\{n\} = S_{k_n} \cap V_{g_v} \cap R_{g_r} \cap L_{g_l}. \tag{2.9}$$

2.1.2 Intrinsic Coordinate Extraction and the Transport Operator ∇_λ

We formalize translation along the three leaf partitions by introducing the direction-dependent transport operator ∇_λ:

Definition 2.1 (Discrete Transport Operator on $\mathbb{N}_2$)**.** Let $n \in \mathbb{N}$ and $s \in \mathbb{Z}$. For a directional parameter $\lambda \in \{0, \frac{1}{2}, 1\}$, the transport operator $\nabla_\lambda(n, s)$ shifts n by s steps along its resident λ-leaf:

$$\text{Trajectory of } \nabla_\lambda(n,s) \subseteq \begin{cases} L_{g_l} & \text{if } \lambda = 0 \quad \text{(Left diagonal leaf)}, \\ V_{g_v} & \text{if } \lambda = 1/2 \quad \text{(Vertical leaf)}, \\ R_{g_r} & \text{if } \lambda = 1 \quad \text{(Right diagonal leaf)}. \end{cases} \tag{2.10}$$

Geometrically, coordinate extraction in $\mathbb{N}_2$ acts as the foliated analogue of orthogonal projection in a Cartesian plane (Figure 2): just as a point in the plane is projected onto coordinate axes to read off its abscissa and ordinate, an integer $n \in \mathbb{N}_2$ is traced backward along its three resident leaves ($\lambda \in \{0, \frac{1}{2}, 1\}$) via ∇_λ until each trajectory terminates at its boundary root. The boundary root reached identifies the leaf generator g_λ, while the number of shells traversed from that root to n measures the local depth d_λ.

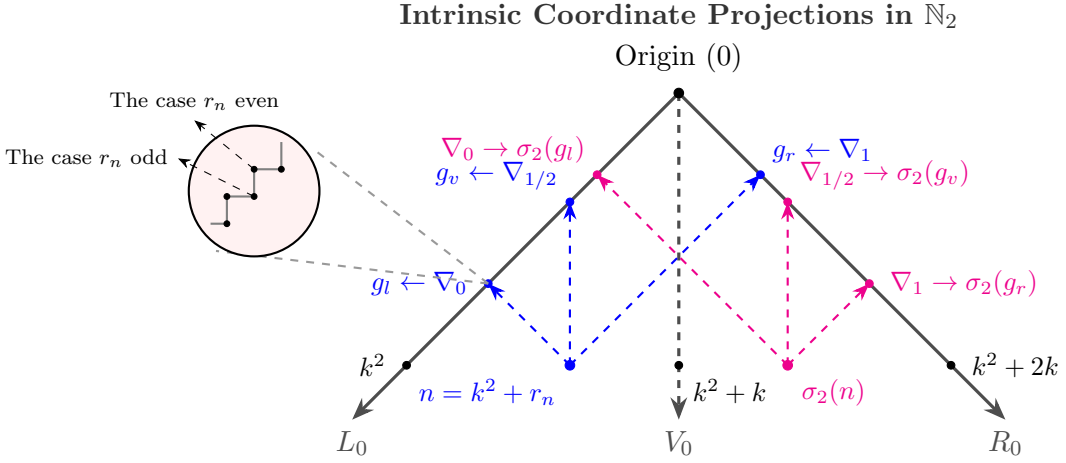


Figure 2: Projection of an integer $n \in \mathbb{N}_2$ along the $\lambda \in \{0, 1/2, 1\}$ leaves back to their boundary roots to extract the intrinsic coordinates (g_λ, d_λ).

Solving Equations (2.4), (2.6), and (2.8) for (g_λ, d_λ) in terms of the shell index $k = \lfloor \sqrt{n} \rfloor$ and residue $r = n - k^2$ yields the closed-form coordinate extraction rules recorded in Table 1, with compact local depths:

$$d_0(n) = k - \left\lceil \frac{r}{2} \right\rceil, \qquad d_{1/2}(n) = k - |r - k|, \qquad d_1(n) = \left\lfloor \frac{r}{2} \right\rfloor. \tag{2.11}$$

Example 2.1 (Coordinate Extraction for $n = 9$ and $n = 10$)**.** For $n = 9$ and $n = 10$, $k = \lfloor \sqrt{n} \rfloor = 3$ with residues $r = 0$ and $r = 1$. Table 1 and Equation (2.11) yield the coordinate representations:

$$9 = (3,0)_S = (0,3)_0 = (-3,0)_{1/2} = (6,0)_1, \qquad 10 = (3,1)_S = (1,2)_0 = (-2,1)_{1/2} = (5,0)_1.$$

Table 1: Coordinate Extraction (Φ_2) for the Quadratic Foliation ($m = 2$). Each integer $n = k^2 + r$ is mapped to its generator g_λ and local leaf depth d_λ across $\lambda \in \{0, \frac{1}{2}, 1\}$.

Leaf Partition	**Algebraic Equation**	**Generator** (g_λ or k)	**Depth** (d_λ or r)
Shell S_k	$n = k^2 + r$	$k = \lfloor \sqrt{n} \rfloor$	$r = n - k^2$
Left Vertical V_{-g} ($\lambda = 1/2$)	$n = (g + d)^2 + d$	$g_v = r - k$	$d_v = r$
Right Vertical V_g ($\lambda = 1/2$)	$n = (g + d)^2 + d + 2g$	$g_v = r - k$	$d_v = 2k - r$
Right Diagonal R_{2g} ($\lambda = 1$)	$n = (g + d)^2 + 2d$	$g_r = 2k - r$	$d_r = \frac{r}{2}$
Right Diagonal R_{2g+1} ($\lambda = 1$)	$n = (g + d + 1)^2 + 2(d + 1) - 1$	$g_r = 2k - r$	$d_r = \frac{r-1}{2}$
Left Diagonal L_{2g} ($\lambda = 0$)	$n = (g + d)^2 + 2g$	$g_l = r$	$d_l = k - \frac{r}{2}$
Left Diagonal L_{2g+1} ($\lambda = 0$)	$n = (g + d + 1)^2 + 2g + 1$	$g_l = r$	$d_l = k - \frac{r+1}{2}$

To transport an integer $n = k^2 + r$ across s shells from $k = \lfloor \sqrt{n} \rfloor$ to target shell $k \pm s$ while preserving its leaf generator g_λ, the intra-shell residue must shift by $r' = r \pm 2\lambda s$. Expanding $(k \pm s)^2 + (r \pm 2\lambda s)$ gives the closed-form quadratic transport operator:

$$\begin{aligned} \nabla_\lambda(n, \pm s) &= (k \pm s)^2 + (r \pm 2\lambda s) \\ &= n \pm 2s\lfloor \sqrt{n} \rfloor + s^2 \pm 2\lambda s. \end{aligned} \tag{2.12}$$

Here $\lambda = 0$ preserves $g_l = r$, $\lambda = 1/2$ preserves $g_v = r - k$, and $\lambda = 1$ preserves $g_r = 2k - r$. Within a fixed shell S_k, horizontal translation reduces to unit succession $r \mapsto r + 1$, whereas crossing from S_k to S_{k+1} is governed by the quadratic expansion of ∇_λ.

2.1.3 1-Zigzag Geodesic Routing and the Chebyshev Metric on $\mathbb{N}_2$

We now define the global geodesic distance $\delta(x, y)$ between any two integers $x, y \in \mathbb{N}_2$. Because legal steps on the lattice follow the leaves of the foliation, the shortest path between $u = \min(x, y)$ and $v = \max(x, y)$ is achieved by at most a 1-zigzag trajectory: a diagonal transport to align the vertical generators ($\Delta g = g_v(v) - g_v(u)$), followed by a vertical transport to align the shell indices ($\Delta k = |k_x - k_y|$).

For $\Delta g \neq 0$, the bounding diagonal direction $\lambda^* \in \{0, 1\}$ toward the target is selected by:

$$\lambda^* = \frac{\Delta g + |\Delta g|}{2|\Delta g|} \in \{0, 1\}. \tag{2.13}$$

Transporting u by $|\Delta g|$ steps along λ^* reaches the intermediate turning point $X(u, v) = \nabla_{\lambda^*}(u, |\Delta g|)$, which resides in shell $\lfloor \sqrt{\nabla_{\lambda^*}(u, |\Delta g|)} \rfloor = \min(k_x, k_y) + |\Delta g|$. Using the identity $\max(A, B) = \frac{1}{2}(A + B + |A - B|)$, the geodesic distance is expressed directly in terms of ∇_{λ^*}:

$$\delta(x, y) = \frac{1}{2}\left(\left(\lfloor \sqrt{v} \rfloor - \lfloor \sqrt{u} \rfloor\right) + |\Delta g| + \left| \lfloor \sqrt{v} \rfloor - \lfloor \sqrt{\nabla_{\lambda^*}(u, |\Delta g|)} \rfloor \right| \right) \tag{2.14}$$

$$= \frac{1}{2}\Big(\Delta k + |\Delta g| + \big| \Delta k - |\Delta g| \big| \Big) = \max(\Delta k, |\Delta g|). \tag{2.15}$$

Equation (2.15) proves that $(\mathbb{N}_2, \delta)$ is a Chebyshev (L^∞) metric space satisfying non-negativity, identity of indiscernibles, symmetry, and the triangle inequality. Because $\delta(x, y) \in \mathbb{N}$, the unit open ball $B_1(x) = \{y \in \mathbb{N}_2 \mid \delta(x, y) < 1\} = \{x\}$ isolates singletons, inducing the discrete topology on $\mathbb{N}_2$.

Remark 2.2. Equation (2.14) demonstrates that the same transport operator ∇_λ that defines foliated arithmetic operations also generates the global L^∞ geodesic metric of the lattice. While $\nabla_{\lambda^*}(u, |\Delta g|)$ serves as the virtual intersection of the diagonal leaf of u with the vertical leaf $V_{g_v(v)}$ of v, the physical turning point along the lattice trajectory is given by the non-overshooting shift $X_{\text{actual}}(u, v) = \nabla_{\lambda^*}\big(u, \min(\Delta k, |\Delta g|)\big)$, which distinguishes two routing regimes:

- **Diagonal-to-Vertical Regime ($\Delta k \geq |\Delta g|$):** The diagonal trajectory from u reaches the vertical leaf $V_{g_v(v)}$ at $X_{\text{actual}}(u, v) = \nabla_{\lambda^*}(u, |\Delta g|)$ in shell $k_u + |\Delta g| \leq k_v$, and the second leg descends the remaining $\Delta k - |\Delta g|$ steps vertically along $\lambda = 1/2$ to reach v.
- **Diagonal-to-Shell Regime ($|\Delta g| > \Delta k$):** The diagonal trajectory from u reaches the target shell S_{k_v} at $X_{\text{actual}}(u, v) = \nabla_{\lambda^*}(u, \Delta k)$ before intersecting $V_{g_v(v)}$, and the absolute-value term $\big|\lfloor\sqrt{v}\rfloor - \lfloor\sqrt{\nabla_{\lambda^*}(u, |\Delta g|)}\rfloor\big| = |\Delta g| - \Delta k$ measures the remaining $|v - X_{\text{actual}}(u, v)|$ horizontal intra-shell steps along S_{k_v} to reach v.

2.2 The m-Degree Foliation ($m > 2$)

2.2.1 Power Shells, Medians, and Leaf Parameterizations

Generalizing the quadratic construction to any integer degree $m > 2$, we partition $\mathbb{N}$ into shells between consecutive m-th powers:

$$S_{k,m} = \big\{k^m,\ k^m + 1,\ \ldots,\ (k+1)^m - 1\big\}, \qquad |S_{k,m}| = (k+1)^m - k^m. \tag{2.16}$$

Because consecutive integers k and $k+1$ have opposite parities, $(k+1)^m - k^m$ is odd for all $m \geq 1$ and $k \in \mathbb{N}$. Every shell $S_{k,m}$ therefore possesses a unique integer median:

$$V_{0,m}(k) = \frac{(k+1)^m + k^m - 1}{2} \in \mathbb{N} \tag{2.17}$$

and a shell-wise reflection involution $\sigma_m : \mathbb{N} \to \mathbb{N}$ given by:

$$\sigma_m(n) = \big(\lfloor \sqrt[m]{n} \rfloor + 1\big)^m + \lfloor \sqrt[m]{n} \rfloor^m - n - 1. \tag{2.18}$$

Aligning the medians $V_{0,m}(k)$ along a central vertical axis defines the principal vertical leaf $V_{0,m}$, with the remaining integers of each shell $S_{k,m}$ arranged laterally as shown in Figure 3.

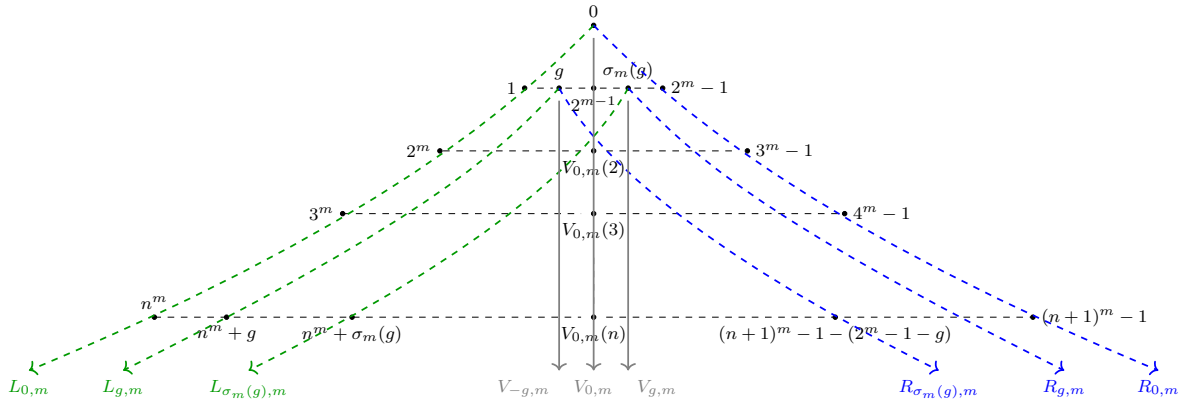


Figure 3: The m-Degree Foliation of Integers: $\mathbb{N}_m$.

Because the cardinality $|S_{\kappa,m}| = (\kappa+1)^m - \kappa^m$ is strictly increasing with $\kappa \in \mathbb{N}$, a leaf indexed by generator g along direction $\lambda \in \{0, \frac{1}{2}, 1\}$ nucleates at a unique minimal *birth shell* $k_0 = k_0(g, \lambda, m)$ where $|S_{\kappa,m}|$ first accommodates the lateral offset g:

$$k_0(g, \lambda, m) = \begin{cases} \inf\left\{\kappa \in \mathbb{N} \;\middle|\; (\kappa+1)^m - \kappa^m > g\right\} & \text{if } \lambda \in \{0, 1\} \quad (g \in \mathbb{N}), \\ \inf\left\{\kappa \in \mathbb{N} \;\middle|\; (\kappa+1)^m - \kappa^m \geq 2|g| + 1\right\} & \text{if } \lambda = \frac{1}{2} \quad (g \in \mathbb{Z}). \end{cases} \tag{2.19}$$

In terms of $k_0 = k_0(g, \lambda, m)$ and local depth $d = k - k_0 \in \mathbb{N}$, the three leaf families are parameterized by:

$$V_{g,m}(d) = \frac{(k_0 + d + 1)^m + (k_0 + d)^m - 1}{2} + g = (k_0 + d)^m + \frac{1}{2}\sum_{i=1}^{m-1} \binom{m}{i}(k_0 + d)^i + g, \quad (2.20)$$

$$L_{g,m}(d) = (k_0 + d)^m + g, \qquad R_{g,m}(d) = \sigma_m\big(L_{g,m}(d)\big) = (k_0 + d + 1)^m - g - 1. \quad (2.21)$$

Theorem 2.3 (Vertical Reflection Symmetry)**.** *For any degree $m \geq 2$, generator $g \in \mathbb{Z}$, and depth $d \in \mathbb{N}$, $\sigma_m\big(V_{g,m}(d)\big) = V_{-g,m}(d)$.*

Proof. Let $n = V_{g,m}(d) \in S_{k,m}$ with $k = k_0 + d = \lfloor \sqrt[m]{n} \rfloor$. Substituting Equation (2.20) into $\sigma_m(n) = (k+1)^m + k^m - n - 1 = 2k^m + \sum_{i=1}^{m-1} \binom{m}{i} k^i - n$ yields:

$$\sigma_m\big(V_{g,m}(d)\big) = 2k^m + \sum_{i=1}^{m-1} \binom{m}{i} k^i - \left[k^m + \frac{1}{2}\sum_{i=1}^{m-1} \binom{m}{i} k^i + g\right] = V_{-g,m}(d).$$

□

2.2.2 Coordinate Extraction, Global Transport, and the Chebyshev Metric in $\mathbb{N}_m$

Inverting Equations (2.20)–(2.21) maps every integer $n \in \mathbb{N}_m$ (with shell index $k = \lfloor \sqrt[m]{n} \rfloor$ and residue $r = n - k^m$) bijectively to its leaf coordinate pair $(g, d)_\lambda$ via the lateral generator

$$g(n, \lambda) = \begin{cases} n - k^m & \text{if } \lambda = 0, \\ n - \frac{(k+1)^m + k^m - 1}{2} & \text{if } \lambda = \frac{1}{2}, \\ (k+1)^m - n - 1 & \text{if } \lambda = 1, \end{cases} \quad (2.22)$$

and the local leaf depth $d_{\lambda,m}(n) = k - k_0\big(g(n, \lambda), \lambda, m\big)$ from Equation (2.19). Throughout the paper, we use the directional subscripts (g_l, g_v, g_r) and (d_l, d_v, d_r) interchangeably with $\big(g(n, 0), g(n, \frac{1}{2}), g(n, 1)\big)$ and $\big(d_{0,m}(n), d_{1/2,m}(n), d_{1,m}(n)\big)$. At $m = 2$, where $|S_{\kappa,2}| = 2\kappa + 1$, Equations (2.19) and (2.22) reduce directly to Table 1 and Equation (2.11).

Example 2.2 (Coordinate Extraction for $m \in \{3, 4\}$)**.** Writing the partitioned coordinate matrix $M_{n,m} = \left[\begin{smallmatrix} k & g_l & g_v & g_r \\ r & d_l & d_v & d_r \end{smallmatrix}\right]$ for $n = 100$ in the cubic ($m = 3$) and quartic ($m = 4$) foliations gives:

$$M_{100,3} = \left[\begin{array}{c|ccc} 4 & 36 & 6 & 24 \\ 36 & 1 & 2 & 1 \end{array}\right], \qquad M_{100,4} = \left[\begin{array}{c|ccc} 3 & 19 & -68 & 155 \\ 19 & 1 & 0 & 0 \end{array}\right].$$

Mathematical Derivation of the m-Degree Transport Operator $\nabla_{\lambda,m}$. To derive the closed-form analytical expression for longitudinal transport across $\mathbb{N}_m$, consider an integer $n \in S_{k,m}$ ($k = \lfloor \sqrt[m]{n} \rfloor$) shifted by $s \geq -d_{\lambda,m}(n)$ shells along its resident λ-leaf to a target integer $n' = \nabla_{\lambda,m}(n, s) \in S_{k+s,m}$. By definition of leaf transport, n and n' share the exact same lateral generator along direction λ:

$$g(n', \lambda) = g(n, \lambda). \quad (2.23)$$

Evaluating the generator invariance condition $g(n', \lambda) = g(n, \lambda)$ between initial shell k and target shell $k' = k + s$ across each of the three canonical directions yields:

- **Left ($\lambda = 0$):** Conserves the distance from the left shell boundary k^m:

$$n' - (k+s)^m = n - k^m \quad \Longrightarrow \quad n' - n = (k+s)^m - k^m \equiv \Delta^{(s)}_{l,m}(k).$$

- **Right ($\lambda = 1$):** Conserves the distance from the right shell boundary $(k+1)^m - 1$:

$$(k+s+1)^m - n' - 1 = (k+1)^m - n - 1 \quad \Longrightarrow \quad n' - n = (k+s+1)^m - (k+1)^m \equiv \Delta^{(s)}_{r,m}(k).$$

- **Vertical ($\lambda = \frac{1}{2}$):** Conserves the signed offset from the median spine $V_{0,m}(k) = \frac{(k+1)^m + k^m - 1}{2}$:

$$n' - \frac{(k+s+1)^m + (k+s)^m - 1}{2} = n - \frac{(k+1)^m + k^m - 1}{2}$$
$$\Longrightarrow \quad n' - n = \frac{1}{2}\Delta^{(s)}_{l,m}(k) + \frac{1}{2}\Delta^{(s)}_{r,m}(k).$$

Because all three directional displacements satisfy the exact convex combination $n' - n = (1-\lambda)\Delta^{(s)}_{l,m}(k) + \lambda\Delta^{(s)}_{r,m}(k)$ for $\lambda \in \{0, \frac{1}{2}, 1\}$, substituting $k = \lfloor \sqrt[m]{n} \rfloor$ yields the unified m-degree transport operator:

$$\nabla_{\lambda,m}(n,s) = n + (1-\lambda)\Big[\big(\lfloor \sqrt[m]{n} \rfloor + s\big)^m - \lfloor \sqrt[m]{n} \rfloor^m \Big] + \lambda\Big[\big(\lfloor \sqrt[m]{n} \rfloor + s + 1\big)^m - \big(\lfloor \sqrt[m]{n} \rfloor + 1\big)^m \Big]. \tag{2.24}$$

Furthermore, since $\nabla_{\lambda,m}(n, s_1)$ lands in shell $k_1 = k + s_1$, applying a subsequent shift s_2 along the same direction λ telescopes the boundary differences:

$$\Delta^{(s_1)}_{\bullet,m}(k) + \Delta^{(s_2)}_{\bullet,m}(k + s_1) = \Big[(k+s_1)^m - k^m\Big] + \Big[(k+s_1+s_2)^m - (k+s_1)^m\Big] = \Delta^{(s_1+s_2)}_{\bullet,m}(k),$$

proving that for all $s_1 \geq -d_{\lambda,m}(n)$ and $s_1 + s_2 \geq -d_{\lambda,m}(n)$, $\nabla_{\lambda,m}$ is strictly step-additive: $\nabla_{\lambda,m}(\nabla_{\lambda,m}(n, s_1), s_2) = \nabla_{\lambda,m}(n, s_1 + s_2)$.

Similarly, for any $x, y \in \mathbb{N}_m$ with $u = \min(x,y)$, $v = \max(x,y)$, $\Delta k = \lfloor \sqrt[m]{v} \rfloor - \lfloor \sqrt[m]{u} \rfloor$, $\Delta g = g_v(v) - g_v(u)$, and bounding direction $\lambda^* = \frac{\Delta g + |\Delta g|}{2|\Delta g|} \in \{0, 1\}$, the 1-zigzag geodesic distance evaluates to:

$$\delta_m(x,y) = \frac{1}{2}\left(\big(\lfloor \sqrt[m]{v} \rfloor - \lfloor \sqrt[m]{u} \rfloor\big) + |\Delta g| + \Big| \lfloor \sqrt[m]{v} \rfloor - \lfloor \sqrt[m]{\nabla_{\lambda^*,m}(u, |\Delta g|)} \rfloor \Big| \right) \tag{2.25}$$

$$= \frac{1}{2}\Big(\Delta k + |\Delta g| + \big| \Delta k - |\Delta g| \big| \Big) = \max(\Delta k, |\Delta g|), \tag{2.26}$$

establishing $(\mathbb{N}_m, \delta_m)$ as a Chebyshev (L^∞) metric space for every $m \geq 2$.

Theorem 2.4 (1-Zigzag Chebyshev Geodesic Metric on $\mathbb{N}_m$)**.** *For any degree $m \geq 2$ and $x, y \in \mathbb{N}_m$, let $u = \min(x,y)$, $v = \max(x,y)$, $\Delta k = \lfloor \sqrt[m]{v} \rfloor - \lfloor \sqrt[m]{u} \rfloor$, $\Delta g = g_v(v) - g_v(u)$, $s^* = \min(\Delta k, |\Delta g|)$, and $\lambda^* = \frac{\Delta g + |\Delta g|}{2|\Delta g|} \in \{0, 1\}$.*

1. ***Global Spine-Coordinate Chebyshev Metric ($m \geq 2$):*** *In the canonical vertical-spine chart (k, g_v), where elementary vertical shifts $\nabla_{1/2,m}(n, \pm 1)$ ($\Delta k = 1, \Delta g_v = 0$) and intra-shell steps $n \pm 1$ ($\Delta k = 0, |\Delta g_v| = 1$) have universal unitary length $\ell_0 = 1$, the 1-zigzag turning point is*

$$X^{(m)}_{\text{actual}}(u,v) = \nabla_{1/2,m}(u, s^*) + \operatorname{sgn}(\Delta g)\, s^*, \tag{2.27}$$

and the global Chebyshev (L^∞) distance is generated analytically by $\nabla_{\lambda^*,m}$ via shell-index telescoping:

$$\delta_m(x,y) = \frac{1}{2}\left(\Delta k + |\Delta g| + \Big| \lfloor \sqrt[m]{v} \rfloor - \lfloor \sqrt[m]{\nabla_{\lambda^*,m}(u, |\Delta g|)} \rfloor \Big| \right)$$
$$= \max(\Delta k, |\Delta g|). \tag{2.28}$$

2. ***Isotropic 3-Leaf Coincidence at*** $m = 2$ ***(Uniqueness of the Quadratic Foliation):*** *At* $m = 2$*, linear shell growth* $|S_{k,2}| = 2k + 1$ *yields* $\nabla_{1/2,2}(u, s) + (2\lambda^* - 1)s = \nabla_{\lambda^*,2}(u, s)$*, so the spine-diagonal turning point coincides identically with boundary-leaf transport,*

$$X^{(2)}_{\text{actual}}(u, v) = \nabla_{\lambda^*,2}\big(u, \min(\Delta k, |\Delta g|)\big), \tag{2.29}$$

and the 3-leaf graph distance (assigning unit length $\ell_0 = 1$ *to* $\nabla_{\lambda,2}(n, \pm 1)$ *across all* $\lambda \in \{0, \frac{1}{2}, 1\}$ *and* $n \pm 1$*) coincides identically with the Chebyshev metric* $\delta_2(x, y) = \max(\Delta k, |\Delta g|)$*. For* $m \geq 3$*, super-linear shell expansion causes single curved-leaf steps* $\nabla_{\lambda,m}(n, \pm 1)$ *(*$\lambda \in \{0, 1\}$*, co-leaf unit length* $\ell_0 = 1$*) to traverse* $|\Delta g_v| = \frac{1}{2}\big(|S_{k+1,m}| - |S_{k,m}|\big) = \mathcal{O}(k^{m-2})$ *vertical columns per shell.*

3 Foliated Arithmetic

3.1 Foliated Addition and Multiplication in $\mathbb{N}_2$ and $\mathbb{N}_m$

In an m-degree foliation $\mathbb{N}_m$ ($m \geq 2$), each base integer a is represented along direction $\lambda \in \{0, \frac{1}{2}, 1\}$ by its coordinate pair $a = (g, d_a)_\lambda$. Foliated addition ($\oplus_m$) advances the local depth of a by b steps along its resident leaves, while foliated multiplication ($\otimes_m$) repeatedly adds the scalar displacement a to the depth $(b - 1)$ times:

$$a \oplus_m b = \big\{\nabla_{\lambda,m}(a, b)\big\}_{\lambda \in \{0,1/2,1\}}, \tag{3.1}$$

$$a \otimes_m b = \big\{\nabla_{\lambda,m}\big(a,\ a(b-1)\big)\big\}_{\lambda \in \{0,1/2,1\}}. \tag{3.2}$$

At $b = 0$, 0 acts as a right-identity for addition ($a \oplus_m 0 = \nabla_{\lambda,m}(a, 0) = a$), whereas adding a to base 0 projects along the three primary boundary leaves ($0 \oplus_2 a = \{a^2, a^2 + a, a^2 + 2a\}$ in $\mathbb{N}_2$). For $m \geq 2$, evaluating $\oplus_m$ across $\lambda \in \{0, \frac{1}{2}, 1\}$ yields multi-valued, non-commutative triads: for instance, $2 \oplus_2 3 = \{17, 20, 23\}$ whereas $3 \oplus_2 2 = \{11, 13, 15\}$ in $\mathbb{N}_2$, and $2 \oplus_3 3 = \{65, 92, 119\}$ whereas $3 \oplus_3 2 = \{29, 44, 59\}$ in $\mathbb{N}_3$.

Example 3.1 (Foliated Multiplication Tables in $\mathbb{N}_2$ and $\mathbb{N}_3$)**.** Evaluating Equation (3.2) across $a, b \in \{1, 2, 3, 4\}$ and $\lambda \in \{0, \frac{1}{2}, 1\}$ generates the directional multiplication tables for the quadratic ($m = 2$) and cubic ($m = 3$) foliations displayed in Table 2. Unlike the symmetric scalar multiplication table of classical $m = 1$ arithmetic, each directional table is asymmetric across its main diagonal ($a \otimes_{\lambda,m} b \neq b \otimes_{\lambda,m} a$).

3.1.1 Cross-Direction Intersections in $\mathbb{N}_2$ vs. Absolute Disjointness for $m \geq 3$

In $\mathbb{N}_2$, a collision $\nabla_{\lambda_1,2}(a, b) = \nabla_{\lambda_2,2}(b, a)$ for $b > a > 0$ cannot occur along the same direction $\lambda_1 = \lambda_2 = \lambda$, since $(b - a)(b + a - 1 + 2\lambda) = 2(ak_b - bk_a)$ has a strictly positive left-hand side and a non-positive right-hand side (k_x/x is decreasing). For $m \geq 3$, even cross-direction intersections are impossible, leaving a single cross-direction additive intersection at $n = 31 \in \mathbb{N}_2$ across all foliations $m \geq 2$:

Theorem 3.1 (Absolute Disjointness for $m \geq 3$)**.** *For any degree* $m \geq 3$ *and all distinct* $a, b \in \mathbb{N}^*$*, the commutative sum triads are strictly disjoint:*

$$(a \oplus_m b) \cap (b \oplus_m a) = \emptyset. \tag{3.3}$$

Proof. Without loss of generality, let $a < b$. Intersecting in a common target shell $K = k_a + b = k_b + a$ requires $b - a = k_b - k_a = 1$, which restricts (a, b) to the shell boundary pair $a = k^m - 1$ ($k_a = k - 1$) and $b = k^m$ ($k_b = k$) for $k \geq 2$, with common target shell $K = k^m + k - 1$.

Table 2: Foliated multiplication tables for the quadratic ($m = 2$) and cubic ($m = 3$) foliations across the three canonical directions $\lambda \in \{0, \frac{1}{2}, 1\}$, illustrating multi-valuedness and non-commutativity ($a \otimes_m b \neq b \otimes_m a$).

Foliated Multiplication Tables

$m = 2$

Left ($\lambda = 0$)

$\otimes_2$	**1**	**2**	**3**	**4**
1	1	4	9	16
2	2	10	26	50
3	3	18	51	102
4	4	36	100	196

Vertical ($\lambda = 1/2$)

$\otimes_2$	**1**	**2**	**3**	**4**
1	1	5	11	19
2	2	12	30	56
3	3	21	57	111
4	4	40	108	208

Right ($\lambda = 1$)

$\otimes_2$	**1**	**2**	**3**	**4**
1	1	6	13	22
2	2	14	34	62
3	3	24	63	120
4	4	44	116	220

$m = 3$

$\otimes_3$	**1**	**2**	**3**	**4**
1	1	8	27	64
2	2	28	126	344
3	3	66	345	1002
4	4	128	732	2200

$\otimes_3$	**1**	**2**	**3**	**4**
1	1	14	42	91
2	2	43	168	425
3	3	93	426	1164
4	4	170	864	2470

$\otimes_3$	**1**	**2**	**3**	**4**
1	1	20	57	118
2	2	58	210	506
3	3	120	507	1326
4	4	212	996	2740

Coincidence on the same direction ($\lambda_1 = \lambda_2$) is impossible because a and b have distinct generators in every direction ($g_l(a) = k^m - (k-1)^m - 1 > 0 = g_l(b)$, $g_v(a) > 0 > g_v(b)$, and $g_r(a) = 0 < (k+1)^m - k^m - 1 = g_r(b)$). For distinct directions ($\lambda_1 \neq \lambda_2$), the directional reference anchors in shell K are separated by multiples of the half-shell span:

$$H_K = \frac{(K+1)^m - K^m - 1}{2},$$

whereas the combined generator offsets of a and b are bounded above by $(k+1)^m - (k-1)^m - 2$. Because $K = k^m + k - 1 \geq 2^m + 1$ for $k \geq 2$, binomial expansion yields the strict inequality:

$$\frac{(K+1)^m - K^m - 1}{2} > (k+1)^m - (k-1)^m - 2 \qquad (\forall\, m \geq 3,\ \forall\, k \geq 2),$$

with the minimal case $m = 3, k = 2$ ($K = 9$) already satisfying $135 > 24$. Thus no cross-direction intersection can occur, and $(a \oplus_m b) \cap (b \oplus_m a) = \emptyset$. □

Corollary 3.2 (Uniqueness of the Cross-Direction Intersection $31 \in \mathbb{N}_2$ Across All Foliations $m > 1$)**.** *Across the entire hierarchy of m-degree integer foliations $\{\mathbb{N}_m\}_{m \geq 2}$ and all non-unit operands $2 \leq a < b$, the prime integer $n = 31 \in S_{5,2}$ in the quadratic foliation ($m = 2$) is the unique cross-direction commutative additive intersection point:*

$$(3 \oplus_2 4) \cap (4 \oplus_2 3) = \{27, \mathbf{31}, 35\} \cap \{25, 28, \mathbf{31}\} = \{\mathbf{31}\}. \tag{3.4}$$

Proof. For $2 \leq a < b$ and $m \geq 2$, target shell coincidence $K = k_a + b = k_b + a$ restricts (a, b) to the consecutive shell boundary pair $a = k^m - 1$ ($k_a = k - 1$) and $b = k^m$ ($k_b = k$) for $k \geq 2$, landing in shell $K = k^m + k - 1$. For $m \geq 3$, Theorem 3.1 establishes $(a \oplus_m b) \cap (b \oplus_m a) = \emptyset$ for all $k \geq 2$. For $m = 2$, $a = k^2 - 1$ has generators $(g_l, g_v, g_r) = (2k - 2,\ k - 1,\ 0)$ and $b = k^2$ has generators $(g_l, g_v, g_r) = (0,\ -k,\ 2k)$. Within shell $K = k^2 + k - 1$, the sole non-trivial cross-direction coincidence occurs between the vertical branch $\nabla_{1/2,2}(a, b) = K(K+1) + (k-1)$ and the right branch $\nabla_{1,2}(b, a) = K(K+2) - 2k$. Equating these two expressions yields:

$$K(K+1) + (k-1) = K(K+2) - 2k \quad \Longleftrightarrow \quad K = 3k - 1 \quad \Longleftrightarrow \quad k^2 - 2k = 0,$$

whose unique solution for $k \geq 2$ is $k = 2$ ($a = 3, b = 4, K = 5$), yielding $\nabla_{1/2,2}(3, 4) = \nabla_{1,2}(4, 3) = 31$. □

Theorem 3.3 (Universal Disjointness of Commutative Products for $m \geq 2$)**.** *For every foliation degree $m \geq 2$ and all distinct $a, b \in \mathbb{N}^*$, the commutative product triads are strictly disjoint:*

$$(a \otimes_m b) \cap (b \otimes_m a) = \emptyset. \tag{3.5}$$

Proof. Without loss of generality, assume $1 \leq a < b$. The product triads $a \otimes_m b = \nabla_{\lambda,m}\big(a, a(b-1)\big)$ and $b \otimes_m a = \nabla_{\lambda,m}\big(b, b(a-1)\big)$ reside entirely within horizontal shells $K_{a,b} = k_a + ab - a$ and $K_{b,a} = k_b + ab - b$, respectively. Since horizontal shells partition $\mathbb{N}_m$, a non-empty intersection requires $K_{a,b} = K_{b,a}$, or equivalently $b - a = k_b - k_a$. If $a = 1$ and $b \geq 2$, then $K_{1,b} = b > \lfloor \sqrt[m]{b} \rfloor = K_{b,1}$ for all $m \geq 2$, so the target shells are strictly disjoint. If $2 \leq a < b$, since consecutive m-th powers are separated by $(k+1)^m - k^m \geq 3$, the condition $b - a = k_b - k_a$ holds only for the adjacent shell-boundary pair $a = k^m - 1$ ($k_a = k - 1$) and $b = k^m$ ($k_b = k$) with $k \geq 2$, which share the common target shell $K = (k-1) + (k^m - 1)^2 = k^{2m} - 2k^m + k$. Because $a = k^m - 1$ is the right boundary of $S_{k-1,m}$ and $b = k^m$ is the left boundary of $S_{k,m}$, their directional generators satisfy $g_l(a) > 0 = g_l(b)$, $g_v(a) > 0 > g_v(b)$, and $g_r(a) = 0 < g_r(b)$. Consequently:

1. **Same-direction Disjointness ($\lambda_1 = \lambda_2$):** Because $g(a, \lambda) \neq g(b, \lambda)$ for every $\lambda \in \{0, \frac{1}{2}, 1\}$, no two branches sharing the same direction can coincide in shell K.

2. **Cross-Direction Disjointness ($\lambda_1 \neq \lambda_2$):** Within shell K, the directional reference anchors ($\lambda \in \{0, \frac{1}{2}, 1\}$) are separated by the half-shell span $H_K = \frac{1}{2}\big((K+1)^m - K^m - 1\big)$, whereas the largest generator offset of a or b toward an adjacent directional anchor is $(k+1)^m - k^m - 1 + \frac{1}{2}\big(k^m - (k-1)^m - 1\big)$. Since $K = k^{2m} - 2k^m + k \geq 10$ for all $m \geq 2$ and $k \geq 2$, we have the strict inequality:

$$H_K = \frac{(K+1)^m - K^m - 1}{2} > (k+1)^m - k^m - 1 + \frac{k^m - (k-1)^m - 1}{2},$$

   where the minimal case $m = 2, k = 2$ ($a = 3, b = 4, K = 10$) already satisfies $H_{10} = 10 > 5$, strictly ordering the six branches in $S_{10,2}$ as $100 < 102 < 108 < 111 < 116 < 120$.

Thus $(a \otimes_m b) \cap (b \otimes_m a) = \emptyset$ for all $m \geq 2$ and all $a \neq b$. □

3.1.2 Non-Distributivity of Foliated Arithmetic

Because leaf depth is decoupled from scalar magnitude, foliated multiplication does not distribute over foliated addition. Comparing $a \otimes_2 (b \oplus_2 c) = \nabla_\lambda\big(a, a(\nabla_\lambda(b, c) - 1)\big)$ and $(a \otimes_2 b) \oplus_2 (a \otimes_2 c) = \nabla_\lambda\big(\nabla_\lambda(a, a(b-1)), \nabla_\lambda(a, a(c-1))\big)$ at $a = b = c = 2$ on $\lambda = 1/2$ gives:

$$2 \otimes_2 (2 \oplus_2 2) = 2 \otimes_2 12 = \nabla_{1/2}(2, 22) = 552,$$
$$(2 \otimes_2 2) \oplus_2 (2 \otimes_2 2) = 12 \oplus_2 12 = \nabla_{1/2}(12, 12) = 240 \neq 552.$$

3.2 The Reflected Double-Lattice $\mathbb{Z}_m$: Subtraction and Four-Quadrant Multiplication

In the non-negative lattice $\mathbb{N}_m$, left multiplication by zero yields $0 \otimes_m a = \nabla_{\lambda,m}(0, 0) = \{0, 0, 0\}$, whereas right multiplication by zero requires a backward shift $a \otimes_m 0 = \nabla_{\lambda,m}(a, -a)$. Since $d_{\lambda,m}(a) \leq \lfloor \sqrt[m]{a} \rfloor < a$ for all $a \geq 2$ and $m \geq 2$, a backward shift of $-a$ overshoots the leaf root $\mathrm{Root}_{\lambda,m}(a) = \nabla_{\lambda,m}\big(a, -d_{\lambda,m}(a)\big)$.

To resolve backward shifts without boundary truncation axioms, we extend $\mathbb{N}_m$ to the planar double-lattice $\mathbb{Z}_m = \mathbb{Z}_m^- \cup \{0\} \cup \mathbb{Z}_m^+$ by reflecting the positive half-lattice $\mathbb{Z}_m^+ = \mathbb{N}_m \setminus \{0\}$ across the origin 0 into a symmetric negative half-lattice $\mathbb{Z}_m^- = -\mathbb{Z}_m^+$. Every non-zero foliated integer $z \in \mathbb{Z}_m^*$ is parameterized by its sign parity $\varepsilon_z = \mathrm{sgn}(z) \in \{-1, +1\}$ and the intrinsic coordinates

of its magnitude $n = |z| \in \mathbb{N}^*$. Because every structural leaf $L_{g,m}, V_{g,m}, R_{g,m}$ in $\mathbb{Z}_m^+$ or $\mathbb{Z}_m^-$ nucleates at a finite birth shell $k_0(g,\lambda,m) \geq 0$ at local depth $d_{\lambda,m}(n) = k_n - k_0(g,\lambda,m)$, an inward shift ($\tilde{s} < 0$) can travel at most $d_{\lambda,m}(n)$ shells within $\mathbb{Z}_m^{\varepsilon_z}$ before reaching its leaf root $\varepsilon_z \operatorname{Root}_{\lambda,m}(n)$. Whenever the inward displacement exceeds this depth ($\tilde{s} < -d_{\lambda,m}(n)$), the trajectory consumes $d_{\lambda,m}(n)$ steps to reach the leaf root $\varepsilon_z \operatorname{Root}_{\lambda,m}(n)$, transitions to the symmetric leaf root $-\varepsilon_z \operatorname{Root}_{\lambda,m}(n)$ in $\mathbb{Z}_m^{-\varepsilon_z}$, and advances outward along that negative leaf by the remaining $|\tilde{s}| - d_{\lambda,m}(n)$ shells.

Definition 3.4 (Extended Discrete Shift Operator on $\mathbb{Z}_m$)**.** Let $z \in \mathbb{Z}_m$ be an arbitrary foliated integer and let $s \in \mathbb{Z}$ be a longitudinal shell shift. For $z \neq 0$, let $\varepsilon_z = \operatorname{sgn}(z) \in \{-1, +1\}$ denote its sign parity, $n = |z| \in \mathbb{N}^*$ its scalar magnitude, $d_{\lambda,m}(n) = k_n - k_0(g,\lambda,m)$ its local leaf depth along direction $\lambda \in \{0, \frac{1}{2}, 1\}$, and $\tilde{s} = \varepsilon_z s$ its oriented step. The extended discrete shift operator $\widehat{\nabla}_{\lambda,m} : \mathbb{Z}_m \times \mathbb{Z} \to \mathbb{Z}_m$ is defined piecewise by:

$$\widehat{\nabla}_{\lambda,m}(z,s) = \begin{cases} 0 & \text{if } z = 0 \text{ and } s = 0, \\ \operatorname{sgn}(s)\Big[(1-\lambda)|s|^m + \lambda\big((|s|+1)^m - 1\big)\Big] & \text{if } z = 0 \text{ and } s \neq 0, \\ \varepsilon_z \, \nabla_{\lambda,m}(n,\, \tilde{s}) & \text{if } z \neq 0 \text{ and } \tilde{s} \geq -d_{\lambda,m}(n), \\ -\varepsilon_z \, \nabla_{\lambda,m}\big(n,\, |\tilde{s}| - 2d_{\lambda,m}(n)\big) & \text{if } z \neq 0 \text{ and } \tilde{s} < -d_{\lambda,m}(n). \end{cases} \tag{3.6}$$

By longitudinal step-additivity along the resident λ-leaf (noting that $|\tilde{s}| - 2d_{\lambda,m}(n) \geq 1 - d_{\lambda,m}(n) > -d_{\lambda,m}(n)$), the fourth branch of Equation (3.6) is identically

$$-\varepsilon_z \, \nabla_{\lambda,m}\big(n,\, |\tilde{s}| - 2d_{\lambda,m}(n)\big) = -\varepsilon_z \, \nabla_{\lambda,m}\Big(\operatorname{Root}_{\lambda,m}(n),\; |\tilde{s}| - d_{\lambda,m}(n)\Big),$$

including on the principal leaves $L_{0,m}, V_{0,m}, R_{0,m}$ where $\operatorname{Root}_{\lambda,m}(n) = 0$.

For any $a, b \in \mathbb{Z}_m$ and $m \geq 2$, foliated addition, subtraction, and multiplication on $\mathbb{Z}_m$ are unified by the extended shift operator across the canonical directional triad $\lambda \in \{0, \frac{1}{2}, 1\}$:

$$a \oplus_m b = \big\{\widehat{\nabla}_{\lambda,m}(a,\, b)\big\}_{\lambda \in \{0,1/2,1\}}, \qquad a \ominus_m b = \big\{\widehat{\nabla}_{\lambda,m}(a,\, -b)\big\}_{\lambda \in \{0,1/2,1\}} = a \oplus_m (-b), \tag{3.7}$$

$$a \otimes_m b = \Big\{\widehat{\nabla}_{\lambda,m}\big(a,\, a(b-1)\big)\Big\}_{\lambda \in \{0,1/2,1\}}. \tag{3.8}$$

In all three operations, the left operand $a \in \mathbb{Z}_m$ acts as the *geometric anchor* (fixing the initial half-lattice $\varepsilon_a = \operatorname{sgn}(a)$ and the resident leaf generator $g(|a|, \lambda)$), whereas the right operand $b \in \mathbb{Z}_m$ acts as the *directed kinematic driver* governing the longitudinal shell displacement.

3.2.1 Four-Quadrant Foliated Addition, Subtraction, and Multiplication

For $a \neq 0$ with $u = |a|$, $v = |b|$, and $\varepsilon_a = \operatorname{sgn}(a)$, the behavior of addition, subtraction, and multiplication across the four quadrants of $\mathbb{Z}_m \times \mathbb{Z}_m$ is governed by the sign of the oriented step $\tilde{s}$ relative to the local leaf-depth threshold $-d_{\lambda,m}(u)$, as summarized in Tables 3 and 4:

- **Addition and Subtraction ($\tilde{s} = \varepsilon_a b$, Table 3):** When a and b share the same sign ($\tilde{s} = +v > 0$), the trajectory advances outward within $\mathbb{Z}_m^{\varepsilon_a}$ to shell $K = k_u + v$. When a and b have opposite signs ($\tilde{s} = -v < 0$, corresponding to subtraction), the trajectory retracts inward within $\mathbb{Z}_m^{\varepsilon_a}$ to shell $K = k_u - v$ if $v \leq d_{\lambda,m}(u)$, and continues across the symmetric leaf root into $\mathbb{Z}_m^{-\varepsilon_a}$ to shell $K = k_u + v - 2d_{\lambda,m}(u) = k_0(g,\lambda,m) + (v - d_{\lambda,m}(u))$ if $v > d_{\lambda,m}(u)$. Because $d_{0,m}(u), d_{1/2,m}(u), d_{1,m}(u)$ generally differ, a single subtraction triad $a \ominus_m v$ can straddle both half-lattices and multiple shells simultaneously.

- **Multiplication ($\tilde{s} = \varepsilon_a \cdot a(b-1) = u(b-1)$, Table 4):** Because $\varepsilon_a^2 = +1$, the oriented multiplicative step $\tilde{s} = u(b-1)$ depends only on $u = |a|$ and the signed multiplier b. For $b \geq 1$, $\tilde{s} = u(v-1) \geq 0$, so the product remains in $\mathbb{Z}_m^{\varepsilon_a}$ at shell $K = k_u + u(v-1)$. For $b \leq -1$ ($v \geq 1$) and any $u \geq 1$, since $d_{\lambda,m}(u) \leq k_u = \lfloor \sqrt[m]{u} \rfloor \leq u < 2u \leq u(v+1)$, the inward step $\tilde{s} = -u(v+1) < -d_{\lambda,m}(u)$ unconditionally exceeds the local leaf depth across all three directions, continuing into $\mathbb{Z}_m^{-\varepsilon_a}$ with net shift $u(v+1) - 2d_{\lambda,m}(u)$. At $b = 0$ ($\tilde{s} = -u$), every anchor $u \geq 2$ likewise satisfies $d_{\lambda,m}(u) \leq \lfloor \sqrt[m]{u} \rfloor < u$ and transitions into $\mathbb{Z}_m^{-\varepsilon_a}$ with shift $u - 2d_{\lambda,m}(u)$, whereas for the unit anchor $u = 1$ ($\tilde{s} = -1$), $\lambda = 0$ ($d_{0,m}(1) = 1$) terminates at 0 while $\lambda \in \{\frac{1}{2}, 1\}$ ($d_{\lambda,m}(1) = 0$) transition into $\mathbb{Z}_m^{-\varepsilon_a}$ with shift 1 (yielding $(\pm 1) \otimes_2 0 = \{0, \mp 5, \mp 6\}$).

Table 3: Operational rules for foliated addition ($a \oplus_m b$) and subtraction ($a \ominus_m b$) on the double-lattice $\mathbb{Z}_m$ across all sign combinations of $a, b \in \mathbb{Z}_m^*$, with $u = |a| \geq 1$, $v = |b| \geq 1$, and local depth $d_\lambda = d_{\lambda,m}(u)$.

Operand Signs $(\varepsilon_a, \varepsilon_b)$	**Foliated Addition** $a \oplus_{\lambda,m} b$	**Foliated Subtraction** $a \ominus_{\lambda,m} b$	**Single-Cone Reduction & Target Shell K (for Addition $a \oplus_{\lambda,m} b$)**
$(+,+)$	$\widehat{\nabla}_{\lambda,m}(+u, +v)$	$\widehat{\nabla}_{\lambda,m}(+u, -v)$	$+\nabla_{\lambda,m}(u, v), \quad K = k_u + v$
$(-,+)$	$\widehat{\nabla}_{\lambda,m}(-u, +v)$	$\widehat{\nabla}_{\lambda,m}(-u, -v)$	$\begin{cases} -\nabla_{\lambda,m}(u, -v), \ K = k_u - v & (v \leq d_\lambda) \\ +\nabla_{\lambda,m}(u, v - 2d_\lambda), \ K = k_u + v - 2d_\lambda & (v > d_\lambda) \end{cases}$
$(-,-)$	$\widehat{\nabla}_{\lambda,m}(-u, -v)$	$\widehat{\nabla}_{\lambda,m}(-u, +v)$	$-\nabla_{\lambda,m}(u, v), \quad K = k_u + v$
$(+,-)$	$\widehat{\nabla}_{\lambda,m}(+u, -v)$	$\widehat{\nabla}_{\lambda,m}(+u, +v)$	$\begin{cases} +\nabla_{\lambda,m}(u, -v), \ K = k_u - v & (v \leq d_\lambda) \\ -\nabla_{\lambda,m}(u, v - 2d_\lambda), \ K = k_u + v - 2d_\lambda & (v > d_\lambda) \end{cases}$
Zero Boundary Rules: $a \oplus_m 0 = a \ominus_m 0 = \{a\}, \quad 0 \oplus_{\lambda,m} b = \widehat{\nabla}_{\lambda,m}(0, b), \quad 0 \ominus_{\lambda,m} b = \widehat{\nabla}_{\lambda,m}(0, -b).$			

Table 4: Operational rules for foliated multiplication ($a \otimes_m b$) on $\mathbb{Z}_m$ across all sign combinations of $a, b \in \mathbb{Z}_m^*$, with $u = |a| \geq 1$, $v = |b| \geq 1$, and local depth $d_\lambda = d_{\lambda,m}(u)$.

Operand Signs $(\varepsilon_a, \varepsilon_b)$	**Oriented Step** $\tilde{s} = \varepsilon_a a(b-1)$	**Extended Transport Formulation**	**Single-Cone Reduction**	**Target Half-Lattice & Shell Index K**
$(+,+)$	$+u(v-1)$	$\widehat{\nabla}_{\lambda,m}(+u, +u(v-1))$	$+\nabla_{\lambda,m}(u, u(v-1))$	$\mathbb{Z}_m^+, \quad k_u + u(v-1)$
$(-,+)$	$+u(v-1)$	$\widehat{\nabla}_{\lambda,m}(-u, -u(v-1))$	$-\nabla_{\lambda,m}(u, u(v-1))$	$\mathbb{Z}_m^-, \quad k_u + u(v-1)$
$(-,-)$	$-u(v+1)$	$\widehat{\nabla}_{\lambda,m}(-u, +u(v+1))$	$+\nabla_{\lambda,m}(u, u(v+1) - 2d_\lambda)$	$\mathbb{Z}_m^+, \quad k_u + u(v+1) - 2d_\lambda$
$(+,-)$	$-u(v+1)$	$\widehat{\nabla}_{\lambda,m}(+u, -u(v+1))$	$-\nabla_{\lambda,m}(u, u(v+1) - 2d_\lambda)$	$\mathbb{Z}_m^-, \quad k_u + u(v+1) - 2d_\lambda$
Zero Rules: $0 \otimes_m b = \{0\}, \quad a \otimes_{\lambda,m} 0 = -\varepsilon_a \nabla_{\lambda,m}(\lvert a\rvert, \lvert a\rvert - 2d_\lambda)$ for $\lvert a\rvert \geq 2, \quad (\pm 1) \otimes_2 0 = \{0, \mp 5, \mp 6\}.$				

Theorem 3.5 (Four-Quadrant Sign, Reflection, and Invertibility Laws on $\mathbb{Z}_m$)**.** *For all $a, b \in \mathbb{Z}_m$ and $\lambda \in \{0, \frac{1}{2}, 1\}$, the four-quadrant foliated operations satisfy the following exact identities:*

1. ***Simultaneous Sign Inversion of Addition and Subtraction:***

$$(-a) \oplus_{\lambda,m} (-b) = -\big(a \oplus_{\lambda,m} b\big), \qquad (-a) \oplus_{\lambda,m} b = -\big(a \ominus_{\lambda,m} b\big). \tag{3.9}$$

2. ***Left-Anchor Sign Linearity of Multiplication:***

$$(-a) \otimes_{\lambda,m} b = -\big(a \otimes_{\lambda,m} b\big). \tag{3.10}$$

3. ***Right-Multiplier Sign Asymmetry*** *($b \geq 1$): For any $a \neq 0$ ($\varepsilon_a = \operatorname{sgn}(a)$) and $b \geq 1$, negating the right multiplier flips the output sign relative to ε_a while shifting the longitudinal shell depth outward by twice the foliated depth deficit $2\big(|a| - d_{\lambda,m}(|a|)\big) \geq 0$:*

$$a \otimes_{\lambda,m} (-b) = -\varepsilon_a \, \nabla_{\lambda,m}\Big(|a \otimes_{\lambda,m} b|,\ 2\big(|a| - d_{\lambda,m}(|a|)\big)\Big). \tag{3.11}$$

4. ***Leaf-Depth Sign Reflection and Subtraction–Addition Invertibility:*** *For every $a \in \mathbb{Z}_m^*$ with $d_{\lambda,m}(|a|) \geq 1$ (and trivially for $a = 0$), shifting inward by twice its local leaf depth reflects a to $-a$:*

$$\widehat{\nabla}_{\lambda,m}\Big(a,\ -2\varepsilon_a d_{\lambda,m}(|a|)\Big) = -a, \tag{3.12}$$

and foliated addition inverts foliated subtraction branch-by-branch for all $b \in \mathbb{Z}$ (also holding at $d_{\lambda,m}(|a|) = 0$ whenever $\varepsilon_a b \leq 0$):

$$\big(a \ominus_{\lambda,m} b\big) \oplus_{\lambda,m} b = a. \tag{3.13}$$

Proof. (1) For $a = 0$, $\widehat{\nabla}_{\lambda,m}(0,-b) = -\widehat{\nabla}_{\lambda,m}(0,b)$ follows directly from the factor $\operatorname{sgn}(s)$ in Definition 3.4. For $a \neq 0$, replacing $(a,b) \mapsto (-a,-b)$ inverts $\varepsilon_{-a} = -\varepsilon_a$ while leaving $n = |-a| = |a|$, $d_{\lambda,m}(n)$, and the oriented shift $\tilde{s} = (-\varepsilon_a)(-b) = \varepsilon_a b$ invariant, negating the output of both $z \neq 0$ branches in Equation (3.6). Replacing $b \mapsto -b$ yields $(-a) \oplus_{\lambda,m} b = -(a \ominus_{\lambda,m} b)$.

(2) In $a \otimes_{\lambda,m} b = \widehat{\nabla}_{\lambda,m}(a, a(b-1))$, replacing $a \mapsto -a$ inverts $\varepsilon_{-a} = -\varepsilon_a$ while keeping $n = |a|$, $d_{\lambda,m}(n)$, and $\tilde{s} = |a|(b-1)$ identical, yielding $(-a) \otimes_{\lambda,m} b = -(a \otimes_{\lambda,m} b)$.

(3) For $a \neq 0$ ($u = |a|$) and $b \geq 1$, we have $|a \otimes_{\lambda,m} b| = \nabla_{\lambda,m}(u, u(b-1))$, whereas $\tilde{s} = -u(b+1) < -d_{\lambda,m}(u)$ gives $a \otimes_{\lambda,m} (-b) = -\varepsilon_a \nabla_{\lambda,m}\big(u, u(b+1) - 2d_{\lambda,m}(u)\big)$. Since $u(b+1) - 2d_{\lambda,m}(u) = u(b-1) + 2(u - d_{\lambda,m}(u))$ with $u - d_{\lambda,m}(u) \geq 0$, longitudinal step-additivity along the resident λ-leaf yields $\nabla_{\lambda,m}\big(u, u(b+1) - 2d_{\lambda,m}(u)\big) = \nabla_{\lambda,m}\big(|a \otimes_{\lambda,m} b|, 2(u - d_{\lambda,m}(u))\big)$.

(4) For $a \in \mathbb{Z}_m^*$ with $d = d_{\lambda,m}(|a|) \geq 1$, setting $s = -2\varepsilon_a d$ gives $\tilde{s} = -2d < -d$, so the fourth branch of Equation (3.6) yields $-\varepsilon_a \nabla_{\lambda,m}(|a|, 2d - 2d) = -\varepsilon_a \nabla_{\lambda,m}(|a|, 0) = -a$. Finally, by (1) it suffices to verify $(a \ominus_{\lambda,m} b) \oplus_{\lambda,m} b = a$ for $a > 0$ with $d = d_{\lambda,m}(a) \geq 1$ and root $O = \nabla_{\lambda,m}(a, -d)$ (for $d = 0$ and $b \leq 0$, $\tilde{s} = -b \geq 0$ stays in $\mathbb{Z}_m^+$). For $b \leq d$, $w = a \ominus_{\lambda,m} b = \nabla_{\lambda,m}(a, -b) \geq 0$ satisfies $w \oplus_{\lambda,m} b = \nabla_{\lambda,m}(w, b) = a$. For $b > d$, $w = a \ominus_{\lambda,m} b = -\nabla_{\lambda,m}(O, b - d) < 0$ has local leaf depth $d_{|w|} = b - d < b$ (since $d \geq 1$); hence $w \oplus_{\lambda,m} b = \widehat{\nabla}_{\lambda,m}(w, b)$ enters the fourth branch with shift $b - 2(b - d) = 2d - b$, giving $+\nabla_{\lambda,m}\big(\nabla_{\lambda,m}(O, b-d), 2d - b\big) = +\nabla_{\lambda,m}(O, d) = a$. □

Example 3.2 (Cross-Origin Subtraction and Four-Quadrant Multiplication in $\mathbb{Z}_2$ and $\mathbb{Z}_3$)**.** Ordering triads by $\lambda \in \{0, \frac{1}{2}, 1\}$:

- **Subtraction in $\mathbb{Z}_2$:** For $13 \ominus_2 2$ ($d_{\lambda,2}(13) = \{1,2,2\}$), $\lambda = 0$ crosses its leaf root $8 \in L_4$ with shift $2 - 2(1) = 0$ while $\lambda \in \{\frac{1}{2}, 1\}$ remain positive, yielding $13 \ominus_2 2 = \{-13, 3, 1\}$. For $12 \ominus_2 3$ ($d_{\lambda,2}(12) = \{1,3,1\}$), $\lambda \in \{0,1\}$ cross their leaf roots $7 \in L_3$ and $5 \in R_3$ with shift $3 - 2(1) = 1$, yielding $12 \ominus_2 3 = \{-19, 0, -21\}$. For $11 \ominus_2 3$ ($d_{\lambda,2}(11) = \{2,2,1\}$), shifts $3 - 2d_{\lambda,2}(11) = \{-1, -1, 1\}$ yield $11 \ominus_2 3 = \{-6, -5, -20\}$.

- **Subtraction in $\mathbb{Z}_3$:** For $n = 10$ ($d_{\lambda,3}(10) = \{1,0,0\}$), we obtain $10 \ominus_3 1 = \{3, -38, -47\}$ and, with shifts $2 - 2\{1,0,0\} = \{0,2,2\}$, $10 \ominus_3 2 = \{-10, -87, -108\}$.

- **Four-Quadrant Multiplication:** In $\mathbb{Z}_2$, since $d_{\lambda,2}(3) = \{0,0,1\}$, we have $3 \otimes_2 5 = \{171, 183, 195\}$, $3 \otimes_2 (-5) = \{-363, -381, -323\}$ (shifts $18 - 2\{0,0,1\} = \{18,18,16\}$), and $3 \otimes_2 0 = \{-18, -21, -8\}$ (shifts $3 - 2\{0,0,1\} = \{3,3,1\}$). In $\mathbb{Z}_3$, since $d_{\lambda,3}(2) = \{0,0,0\}$, we have $2 \otimes_3 3 = \{126, 168, 210\}$, $2 \otimes_3 (-2) = \{-344, -425, -506\}$, and $2 \otimes_3 0 = \{-28, -43, -58\}$.

3.2.2 Foliated Exponentiation: Leaf-Conserving and Left-Recursive Powers

In classical Peano arithmetic ($m = 1$), exponentiation a^p is uniquely defined by repeated scalar multiplication. For $m \geq 2$, the non-commutativity and non-associativity of $\otimes_{\lambda,m}$—which decouples the left geometric leaf-anchor from the right kinematic stride multiplier—induces two distinct, geometrically meaningful exponentiation operators depending on whether iteration preserves the initial leaf of the base a or compounds across shells recursively.

Definition 3.6 (Leaf-Conserving Foliated Power)**.** Let $a \in \mathbb{N}_m^*$ be a base integer with intrinsic coordinates $(g, d_a)_\lambda$ along direction $\lambda \in \{0, \frac{1}{2}, 1\}$, and let $p \in \mathbb{N}^*$ be a positive integer exponent. Anchoring a permanently on the left and iterating the multiplicative stride $a \otimes_{\lambda,m} a^{p-1}$ defines the *leaf-conserving foliated p-th power* $a^{\langle p\rangle_m} = \{a^{\langle p\rangle_{\lambda,m}}\}_{\lambda\in\{0,1/2,1\}}$ by:

$$a^{\langle p\rangle_{\lambda,m}} \equiv a \otimes_{\lambda,m} a^{p-1} = \big(g,\, d_a + a^p - a\big)_\lambda = \nabla_{\lambda,m}\big(a,\, a^p - a\big). \tag{3.14}$$

Extending Equation (3.14) to the zero exponent ($p = 0$) on the planar double-lattice $\mathbb{Z}_m$ via the extended shift operator $\widehat{\nabla}_{\lambda,m}$ yields:

$$a^{\langle 0\rangle_{\lambda,m}} \equiv \widehat{\nabla}_{\lambda,m}\big(a,\, 1 - a\big). \tag{3.15}$$

Remark 3.7 (Left-Recursive Foliated Power)**.** Alternatively, feeding the multi-valued output of each foliated multiplication back into the left anchor slot defines the *left-recursive foliated power* $a^{[p]_{\lambda,m}}$ inductively via $a^{[1]_{\lambda,m}} = a$ and:

$$a^{[p+1]_{\lambda,m}} \equiv a^{[p]_{\lambda,m}} \otimes_{\lambda,m} a = \nabla_{\lambda,m}\Big(a^{[p]_{\lambda,m}},\, a^{[p]_{\lambda,m}}(a-1)\Big) \qquad (p \geq 1). \tag{3.16}$$

While both formulations coincide at the foliated square ($a^{\langle 2\rangle_{\lambda,m}} = a^{[2]_{\lambda,m}} = a \otimes_{\lambda,m} a = \nabla_{\lambda,m}(a, a^2 - a)$) and remain on the same λ-leaf $g(a, \lambda)$ by step-additivity, the recursive shell depth grows super-exponentially as a tower of degree m^p, whereas the leaf-conserving power $a^{\langle p\rangle_{\lambda,m}}$ advances the shell index by the exact polynomial stride $s = a^p - a$.

Proposition 3.8 (Algebraic and Geometric Laws of Leaf-Conserving Powers)**.** *For every base $a \in \mathbb{N}_m^*$, exponents $p, q \in \mathbb{N}^*$, and direction $\lambda \in \{0, \frac{1}{2}, 1\}$, the leaf-conserving foliated power satisfies:*

1. ***Generator Conservation and Shell Index:*** *All powers $\{a^{\langle p\rangle_{\lambda,m}}\}_{p\geq 1}$ inhabit the common structural leaf $g\big(a^{\langle p\rangle_{\lambda,m}}, \lambda\big) = g(a, \lambda)$ at longitudinal shell index:*

$$k\Big(a^{\langle p\rangle_{\lambda,m}}\Big) = k_a + a^p - a. \tag{3.17}$$

2. ***Exact Quotient Reduction:*** *Under exact foliated division $\oslash_{\lambda,m}$ by the base a, the foliated p-th power reduces to the classical $(p-1)$-th scalar power:*

$$a^{\langle p\rangle_{\lambda,m}} \oslash_{\lambda,m} a = 1 + \frac{k\big(a^{\langle p\rangle_{\lambda,m}}\big) - k_a}{a} = 1 + \frac{a^p - a}{a} = a^{p-1}. \tag{3.18}$$

3. ***Additive Step Composition of Successive Powers:*** *Transporting $a^{\langle p\rangle_{\lambda,m}}$ along its resident λ-leaf by $a^p(a^q - 1)$ shells recovers the $(p+q)$-th foliated power:*

$$\nabla_{\lambda,m}\Big(a^{\langle p\rangle_{\lambda,m}},\, a^p(a^q - 1)\Big) = a^{\langle p+q\rangle_{\lambda,m}}. \tag{3.19}$$

4. ***Peano Correspondence*** *($m = 1$)**:*** *At the flat limit $m = 1$, where $\nabla_{\lambda,1}(a, s) = a + s$, Equations (3.14)–(3.15) collapse identically to classical scalar exponentiation:*

$$a^{\langle p\rangle_{\lambda,1}} = a + (a^p - a) = a^p \quad (p \geq 1), \qquad a^{\langle 0\rangle_{\lambda,1}} = a + (1 - a) = 1. \tag{3.20}$$

Example 3.3 (Foliated Powers of $a = 2$ and $a = 3$ in $\mathbb{N}_2$ and $\mathbb{N}_3$)**.** Ordering directional triads by $\lambda \in \{0, \frac{1}{2}, 1\}$:

- **In the Quadratic Foliation $\mathbb{N}_2$ ($m = 2$):** For $a = 2$ ($k_2 = 1$), the first three leaf-conserving powers are:

$$\begin{aligned} 2^{\langle 1\rangle_2} &= \nabla_{\lambda,2}(2,\,0) = \{2, 2, 2\} \quad (k = 1), \\ 2^{\langle 2\rangle_2} &= 2 \otimes_2 2 = \nabla_{\lambda,2}(2,\,2) = \{10, 12, 14\} \quad (k = 3), \\ 2^{\langle 3\rangle_2} &= 2 \otimes_2 4 = \nabla_{\lambda,2}(2,\,6) = \{50, 56, 62\} \quad (k = 7), \end{aligned}$$

  whereas the zero power in $\mathbb{Z}_2$ evaluates to $2^{\langle 0\rangle_2} = \widehat{\nabla}_{\lambda,2}(2, -1) = \{-5, 0, 0\}$. For $a = 3$ ($k_3 = 1$), $3^{\langle 2\rangle_2} = \nabla_{\lambda,2}(3, 6) = \{51, 57, 63\}$ ($k = 7$) and $3^{\langle 3\rangle_2} = \nabla_{\lambda,2}(3, 24) = \{627, 651, 675\}$ ($k = 25$).

- **In the Cubic Foliation $\mathbb{N}_3$ ($m = 3$):** For $a = 2$ ($k_2 = 1$), $2^{\langle 2\rangle_3} = \nabla_{\lambda,3}(2, 2) = \{28, 43, 58\}$ ($k = 3$) and $2^{\langle 3\rangle_3} = \nabla_{\lambda,3}(2, 6) = \{344, 425, 506\}$ ($k = 7$).

3.3 Foliated Euclidean Division and Modular Arithmetic

Inverting the foliated multiplication operator $a \otimes_{\lambda,m} q = \nabla_{\lambda,m}\big(a, a(q-1)\big)$ defines directional Euclidean division ($\oslash_{\lambda,m}$) and modularity ($\mathrm{mod}_{\lambda,m}$) on $\mathbb{N}_m$.

Definition 3.9 (Exact Foliated Divisibility and Quotient $\oslash_{\lambda,m}$)**.** Let $N \in \mathbb{N}_m$ ($k_N = \lfloor \sqrt[m]{N} \rfloor$) and $a \in \mathbb{N}^*$ ($k_a = \lfloor \sqrt[m]{a} \rfloor \le k_N$). The dividend N is **foliated-divisible** by a along direction $\lambda \in \{0, \frac{1}{2}, 1\}$, denoted $a \mid_{\lambda,m} N$, if and only if there exists $q \in \mathbb{N}^*$ such that $N = a \otimes_{\lambda,m} q = \nabla_{\lambda,m}\big(a, a(q-1)\big)$. Equivalently:

$$a \mid_{\lambda,m} N \quad \Longleftrightarrow \quad g(N,\lambda) = g(a,\lambda) \quad \text{and} \quad k_N - k_a \equiv 0 \pmod{a}. \tag{3.21}$$

Whenever $a \mid_{\lambda,m} N$, the **Exact Foliated Quotient** is given by:

$$N \oslash_{\lambda,m} a = 1 + \frac{k_N - k_a}{a} = 1 + \frac{d_{\lambda,m}(N) - d_{\lambda,m}(a)}{a}, \tag{3.22}$$

satisfying $(a \otimes_{\lambda,m} q) \oslash_{\lambda,m} a = q$.

Theorem 3.10 (Foliated Euclidean Division Theorem)**.** *For any dividend $N \in \mathbb{N}_m$ and divisor $a \in \mathbb{N}^*$ with $k_N \ge k_a$, and for any direction $\lambda \in \{0, \frac{1}{2}, 1\}$, there exist a unique integer **Foliated Quotient** $q \in \mathbb{N}^*$ and a unique **Foliated Modular Remainder** pair $(\rho_k, \rho_{\lambda,m}) \in \{0, 1, \ldots, a-1\} \times \mathbb{Z}$ such that:*

$$N = \nabla_{\lambda,m}\big(a \otimes_{\lambda,m} q,\ \rho_k\big) + \rho_{\lambda,m} = \nabla_{\lambda,m}\big(a,\ a(q-1) + \rho_k\big) + \rho_{\lambda,m}, \tag{3.23}$$

where:

$$q(N,a) = 1 + \left\lfloor \frac{k_N - k_a}{a} \right\rfloor, \tag{3.24}$$

$$\rho_k(N,a) = (k_N - k_a) \bmod a = (k_N - k_a) - a(q-1) \in \{0, 1, \ldots, a-1\}, \tag{3.25}$$

$$\rho_{\lambda,m}(N,a) = N - \nabla_{\lambda,m}(a,\ k_N - k_a) = \begin{cases} g(N,\lambda) - g(a,\lambda) & \text{if } \lambda \in \{0, \frac{1}{2}\}, \\ g(a,1) - g(N,1) & \text{if } \lambda = 1. \end{cases} \tag{3.26}$$

In particular, $a \mid_{\lambda,m} N \iff N \bmod {}_{\lambda,m} a \equiv \big(\rho_k(N,a),\ \rho_{\lambda,m}(N,a)\big) = (0,0)$.

Proof. Applying Euclidean division to $\Delta k = k_N - k_a \geq 0$ by $a \geq 1$ gives unique integers $q' = \lfloor \Delta k/a \rfloor \geq 0$ and $\rho_k = \Delta k \bmod a \in \{0, \ldots, a-1\}$ with $k_N - k_a = aq' + \rho_k = a(q-1) + \rho_k$ for $q = 1+q'$. By the step-additivity of $\nabla_{\lambda,m}$, transporting $A_\lambda = a \otimes_{\lambda,m} q = \nabla_{\lambda,m}(a, a(q-1))$ by ρ_k steps reaches $\nabla_{\lambda,m}(a, k_N - k_a) \in S_{k_N,m}$, whose intra-shell difference from N is $\rho_{\lambda,m}(N, a) = N - \nabla_{\lambda,m}(a, k_N - k_a)$. □

Example 3.4 (Foliated Division and Modularity)**.** For $N_\lambda \in \{26, 30, 34\} \subset S_5$ divided by $a = 2$ ($k_2 = 1$) in $\mathbb{N}_2$, $N_\lambda \oslash_{\lambda,2} 2 = 1 + (5-1)/2 = 3$ with remainder $(0, 0)$. For $N = 33 \in S_5$ divided by $a = 2$, $q(33, 2) = 3$, $\rho_k(33, 2) = 0$, and $\rho_{\lambda,2}(33, 2) = 33 - (2 \otimes_{\lambda,2} 3) \in \{+7, +3, -1\}$, so $33 \bmod_2 2 = \{(0, +7)_0, (0, +3)_{1/2}, (0, -1)_1\}$.

Remark 3.11 (Left Divisibility vs. Right Multiplier Divisibility)**.** Because foliated multiplication $a \otimes_{\lambda,m} q = N$ is non-commutative, it induces two distinct inverse relations: **left divisibility** ($a \mid^L_{\lambda,m} N$, where the base leaf-anchor a is fixed and q is the unknown stride count) and **right divisibility** ($q \mid^R_{\lambda,m} N$, where the multiplier q is fixed and the co-leaf base a is the unknown). Because the transport operator $\nabla_{\lambda,m}\big(a, a(q-1)\big)$ preserves the generator of the left factor ($g(N, \lambda) = g(a, \lambda)$) and advances the shell index linearly in q with constant period a, left divisibility is the natural leaf-conserving operation that admits a Euclidean division algorithm and modular congruence. Conversely, fixing the right factor q across varying bases a jumps across distinct leaves and yields a degree-m polynomial condition $k_a + a(q-1) = k_N$ for k_a. Notably, for primality classification (Section 3.4), an integer $p > 1$ admits a non-trivial left divisor $a > 1$ if and only if it admits a non-trivial right divisor $q \geq 2$, leaving the prime sets $\mathbb{P}_{\lambda,m}$ invariant.

Definition 3.12 (Foliated Modular Congruence)**.** Two integers $x, y \in \mathbb{N}_m$ are **foliated-congruent modulo** a along direction $\lambda \in \{0, \frac{1}{2}, 1\}$, denoted $x \equiv_{\lambda,m} y \pmod a$, if and only if they inhabit the same λ-leaf ($g(x, \lambda) = g(y, \lambda)$) and have congruent shell indices ($k_x \equiv k_y \pmod a$), or equivalently $y = \nabla_{\lambda,m}(x,\, q \cdot a)$ for some $q \in \mathbb{Z}$.

Proposition 3.13 (Foliated Modular Compatibility on $\mathbb{N}_m$)**.** *Let $a \in \mathbb{N}^*$ be a modulus and let $\lambda \in \{0, \frac{1}{2}, 1\}$. Whenever $x \equiv_{\lambda,m} y \pmod a$, foliated addition and multiplication satisfy:*

1. ***Additive Compatibility:*** *For any longitudinal shifts $s_1, s_2 \in \mathbb{N}$ satisfying $s_1 \equiv s_2 \pmod a$,*
$$x \oplus_{\lambda,m} s_1 \equiv_{\lambda,m} y \oplus_{\lambda,m} s_2 \pmod a. \tag{3.27}$$
2. ***Multiplicative Compatibility:*** *For any multipliers $b_1, b_2 \in \mathbb{N}^*$ satisfying $b_1 \equiv b_2 \pmod a$,*
$$x \otimes_{\lambda,m} b_1 \equiv_{\lambda,m} y \otimes_{\lambda,m} b_2 \pmod a \tag{3.28}$$
holds unconditionally for the boundary directions $\lambda \in \{0, 1\}$, and holds for the central one $\lambda = \frac{1}{2}$ whenever a is odd or $b_1 \equiv b_2 \equiv 1 \pmod 2$.

Proof. Since $\nabla_{\lambda,m}$ preserves the generator of the left anchor, all terms in (1) and (2) inhabit the common leaf $g(x, \lambda) = g(y, \lambda)$. (1) The target shell indices satisfy $k_{x \oplus s_1} - k_{y \oplus s_2} = (k_x - k_y) + (s_1 - s_2) \equiv 0 \pmod a$. (2) The target shell difference is $k_{x \otimes b_1} - k_{y \otimes b_2} = (k_x - k_y) + x(b_1 - b_2) + (x - y)(b_2 - 1) \equiv (x - y)(b_2 - 1) \pmod a$. Because $g(x, \lambda) = g(y, \lambda)$, we have $x - y = (1-\lambda)(k_x^m - k_y^m) + \lambda\big((k_x+1)^m - (k_y+1)^m\big)$. Since $(k_x - k_y)$ algebraically divides both $k_x^m - k_y^m$ and $(k_x+1)^m - (k_y+1)^m$, the condition $a \mid (k_x - k_y)$ implies $a \mid (x - y)$ for $\lambda \in \{0, 1\}$, and for $\lambda = \frac{1}{2}$ whenever $\gcd(a, 2) = 1$ or $2 \mid (b_2 - 1)$. □

3.4 Direction-Dependent Foliated Primality

In $\mathbb{N}_m$ ($m \geq 2$), every integer n sits at the intersection of three leaves and therefore possesses a **Depth Triad**:
$$\mathbf{d}_m(n) = \Big(d_{0,m}(n),\ d_{1/2,m}(n),\ d_{1,m}(n)\Big) \in \mathbb{N}^3. \tag{3.29}$$

Because local leaf depth $d_{\lambda,m}(a)$ is decoupled from scalar magnitude a, primality along a leaf admits two complementary definitions depending on whether the transport step is scaled by the global magnitude a or by the local depth $d_{\lambda,m}(a)$.

3.4.1 Global λ-Foliated Primality (Irreducibility Under $\otimes_{\lambda,m}$)

Definition 3.14 (Global λ-Foliated Primality)**.** An integer $p \in \mathbb{N}_m \setminus \{0,1\}$ is a **global λ-foliated prime** along direction $\lambda \in \{0, \frac{1}{2}, 1\}$ (denoted $p \in \mathbb{P}_{\lambda,m}$) if and only if for every $a \in \mathbb{N}_m \setminus \{0,1\}$ satisfying $g(a,\lambda) = g(p,\lambda)$ (co-leaf alignment) and $d_{\lambda,m}(a) < d_{\lambda,m}(p)$ (shallower depth), the multiplicative transport equation

$$\nabla_{\lambda,m}\big(a,\, (x-1)\cdot a\big) = p \qquad \big(\text{equivalently, } a \otimes_{\lambda,m} x = p\big) \tag{3.30}$$

has no solution $x \in \mathbb{N}$. Otherwise, p is a **global λ-foliated composite** ($p \in \mathbb{K}_{\lambda,m}$). An integer $p > 1$ that is λ-foliated prime across all three directions is an **Omni-Directional Foliated Prime**: $p \in \mathbb{P}_{*,m} \equiv \mathbb{P}_{0,m} \cap \mathbb{P}_{1/2,m} \cap \mathbb{P}_{1,m}$.

By Theorem 3.10, Equation (3.30) has a solution $x \geq 2$ for a co-leaf integer $a > 1$ if and only if $d_{\lambda,m}(p) - d_{\lambda,m}(a) = k_p - k_a \equiv 0 \pmod{a}$. Every leaf root $p > 1$ ($d_{\lambda,m}(p) = 0$) is automatically in $\mathbb{P}_{\lambda,m}$.

Theorem 3.15 (Direction-Relativity of Global Foliated Primality)**.** *For every $m \geq 2$ and $\lambda_1 \neq \lambda_2$, $\mathbb{P}_{\lambda_1,m} \cap \mathbb{K}_{\lambda_2,m} \neq \emptyset$.*

Proof. In $\mathbb{N}_2$, for every $x \geq 2$, the element $n_x = 2 \otimes_{1/2,2} x = \nabla_{1/2}(2, 2x-2) \in S_{2x-1}$ is composite on $\lambda = 1/2$ ($n_x \in \mathbb{K}_{1/2,2}$). On $\lambda = 0$, $g_l(n_x) = 2x - 1$ has birth shell $k_0 = x$, so any shallower element $a' > 1$ on L_{2x-1} satisfies $k_{a'} \geq x \geq 2$ and $a' \geq x^2 > x - 1 \geq k_{n_x} - k_{a'} > 0$, making $k_{n_x} \equiv k_{a'} \pmod{a'}$ impossible (and identically on $\lambda = 1$). Thus $n_x \in (\mathbb{P}_{0,2} \cap \mathbb{P}_{1,2}) \cap \mathbb{K}_{1/2,2}$ for all $x \geq 2$ (and similarly for $m > 2$). □

From Extrinsic Scalar Strides to Intrinsic Leaf-Depth Primality. In classical Peano arithmetic ($m = 1$), the scalar magnitude of an integer $a \in \mathbb{N}$ and its coordinate depth from the origin are identical ($d_{\lambda,1}(a) = a$). For $m \geq 2$, however, global scalar magnitude $a \sim k_a^m$ and local leaf depth $d_{\lambda,m}(a) = k_a - k_0(g,\lambda,m)$ decouple completely. While Definition 3.14 characterizes algebraic irreducibility under the global product $\otimes_{\lambda,m}$, it scales the longitudinal step size $(x-1)\cdot a$ by the *extrinsic scalar magnitude* a rather than by the intrinsic geometry of the host leaf. Because $a \sim k_a^m$ grows polynomial-fold faster than the shell index k_a, the global sieve jumps across shells with rapidly diverging strides $s = (x-1)a$, leaving the vast majority of integers unsieved and importing an external scalar label into a purely one-dimensional leaf trajectory.

To achieve a purely intrinsic geometric classification, a structural leaf $L_{g,m}$, $V_{g,m}$, or $R_{g,m}$ must be treated as an autonomous one-dimensional Peano half-line originating at its own birth shell $k_0(g,\lambda,m)$. Along any fixed leaf, the true coordinate distance of an element a from its leaf root is its local depth $d_{\lambda,m}(a) \in \mathbb{N}$, not its ambient scalar value a. Replacing the extrinsic scalar stride $(x-1)\cdot a$ with the *intrinsic depth-scaled stride* $(x-1)\cdot d_{\lambda,m}(a)$ establishes an exact, scale-invariant isomorphism between each leaf and the classical integers $\mathbb{N}$, where the leaf root ($d = 0$) acts as the local zero, the first step ($d = 1$) acts as the local unit, and irreducibility is governed strictly by the divisibility of the intrinsic coordinate $d_{\lambda,m}(n)$. This second formulation is geometrically more accurate because it depends exclusively on the internal metric of the foliation and directly drives the exact holographic conservation laws developed in Section 4.

3.4.2 Local Leaf-Depth Primality and Intrinsic Leaf Classification

Scaling the transport step by the local coordinate $d_{\lambda,m}(a)$ instead of a characterizes primality purely within the internal 1D sequence of a single leaf:

Definition 3.16 (Local Leaf-Depth Primality and Leaf Classification)**.** Along direction $\lambda \in \{0, \frac{1}{2}, 1\}$ in $\mathbb{N}_m$, an integer $p \in \mathbb{N}_m$ with $d_{\lambda,m}(p) > 1$ is **locally leaf-depth prime** (denoted $p \in \mathcal{D}_{\lambda,m}$) if and only if for every shallower co-leaf integer $a \in \mathbb{N}_m$ satisfying $g(a, \lambda) = g(p, \lambda)$ and $1 < d_{\lambda,m}(a) < d_{\lambda,m}(p)$, the local transport equation

$$\nabla_{\lambda,m}\Big(a,\ (x-1) \cdot d_{\lambda,m}(a)\Big) = p \tag{3.31}$$

has no solution $x \in \mathbb{N}$. Every integer $n \in \mathbb{N}_m$ falls into one of four classes along its λ-leaf:

1. λ**-Leaf Root:** $d_{\lambda,m}(n) = 0$.
2. λ**-Leaf Unit:** $d_{\lambda,m}(n) = 1$.
3. λ**-Prime-Depth Element** ($n \in \mathcal{D}_{\lambda,m}$)**:** $d_{\lambda,m}(n) \in \mathbb{P} = \{2, 3, 5, 7, \dots\}$.
4. λ**-Composite-Depth Element** ($n \in \mathcal{C}_{\lambda,m}$)**:** $d_{\lambda,m}(n) \in \mathbb{K} = \{4, 6, 8, 9, \dots\}$.

An integer satisfying $\mathbf{d}_m(n) \in \mathbb{P}^3$ is an **Omni-Directional Prime-Depth Element** (or **Triple Leaf-Depth Prime**, $n \in \mathcal{D}_{*,m}$).

Proposition 3.17 (Equivalence to Prime Local Depth)**.** *Equation* (3.31) *has no solution* $x \in \mathbb{N}$ *across all co-leaf integers* a *with* $1 < d_{\lambda,m}(a) < d_{\lambda,m}(p)$ *if and only if* $d_{\lambda,m}(p) \in \mathbb{P}$.

Proof. Along a fixed λ-leaf, $d_{\lambda,m}(\nabla_{\lambda,m}(a, s)) = d_{\lambda,m}(a) + s$. Setting $s = (x-1) \cdot d_{\lambda,m}(a)$ gives $d_{\lambda,m}(p) = x \cdot d_{\lambda,m}(a)$, which admits no solution $x \geq 2$ for $1 < d_{\lambda,m}(a) < d_{\lambda,m}(p)$ if and only if $d_{\lambda,m}(p) \in \mathbb{P}$. □

Example 3.5 (Global vs. Local Leaf-Depth Primality)**.** In $\mathbb{N}_2$, $n = 29$ ($k = 5, r = 4$) is an Omni-Directional Foliated Prime ($29 \in \mathbb{P}_{*,2}$) under Definition 3.14, while its depth triad $\mathbf{d}_2(29) = (3, 4, 2)$ places it in $\mathcal{D}_{0,2} \cap \mathcal{D}_{1,2} \cap \mathcal{C}_{1/2,2}$. Conversely, $n = 30 = 2 \otimes_{1/2,2} 3$ is globally composite on $\lambda = 1/2$ ($30 \in \mathbb{K}_{1/2,2}$), yet its depth triad $\mathbf{d}_2(30) = (2, 5, 2) \in \mathbb{P}^3$ places it in $\mathcal{D}_{*,2}$.

Theorem 3.18 (Intrinsic Leaf-Depth Fermat Little Theorem on $\mathbb{N}_m$)**.** *Let* $\lambda \in \{0, \frac{1}{2}, 1\}$ *and let* $q \in \mathcal{D}_{\lambda,m}$ *be a local leaf-depth prime, so that its intrinsic depth* $\delta_q = d_{\lambda,m}(q) \in \mathbb{P}$ *is prime. For any integer* $x \in \mathbb{N}_m$ *with local depth* $d_x = d_{\lambda,m}(x)$*, define the intrinsic leaf-depth power along direction* λ *by:*

$$x^{\langle q \rangle^{\mathrm{loc}}_{\lambda,m}} \equiv \nabla_{\lambda,m}\Big(x,\ d_x^{\delta_q} - d_x\Big). \tag{3.32}$$

Then $x^{\langle q \rangle^{\mathrm{loc}}_{\lambda,m}}$ *preserves the resident leaf generator* $g(x, \lambda)$ *and satisfies the exact intrinsic congruence:*

$$x^{\langle q \rangle^{\mathrm{loc}}_{\lambda,m}} \equiv_{\lambda,m} x \pmod{d_{\lambda,m}(q)}. \tag{3.33}$$

Proof. By definition of $\nabla_{\lambda,m}$, $x^{\langle q \rangle^{\mathrm{loc}}_{\lambda,m}}$ and x share the same generator $g(x, \lambda)$ and birth shell $k_0(g(x, \lambda), \lambda, m)$. Since $q \in \mathcal{D}_{\lambda,m}$, $\delta_q = d_{\lambda,m}(q)$ is prime, so δ_q divides $d_x^{\delta_q} - d_x$ for every $d_x \in \mathbb{N}$. Consequently, the shell index difference is $k\Big(x^{\langle q \rangle^{\mathrm{loc}}_{\lambda,m}}\Big) - k_x = d_x^{\delta_q} - d_x \equiv 0 \pmod{d_{\lambda,m}(q)}$. □

3.4.3 Leaf-Local Fundamental Theorem of Arithmetic and Triadic Coupling

Whereas global scalar primes $\mathbb{P}$ are distributed across horizontal shells without internal multiplicative closure along individual leaves, local leaf-depth primality $\mathcal{D}_{\lambda,m}$ endows every structural leaf $\mathcal{L}_{g,\lambda} \in \{L_{g,m}, V_{g,m}, R_{g,m}\}$ (for $\lambda = 0, \frac{1}{2}, 1$, respectively) with an autonomous unique factorization structure. This establishes a direct algebraic bridge between the longitudinal geometry of the foliation and the multiplicative structure of the integers.

Definition 3.19 (Intrinsic Co-Leaf Multiplication)**.** Fix a foliation degree $m \geq 1$, a direction $\lambda \in \{0, \frac{1}{2}, 1\}$, and a structural leaf $\mathcal{L}_{g,\lambda} = \{(g,d)_\lambda\}_{d\in\mathbb{N}}$ originating at birth shell $k_0 = k_0(g,\lambda,m)$. For any two co-leaf elements $x, y \in \mathcal{L}_{g,\lambda}$ with local depths $d_x = d_{\lambda,m}(x)$ and $d_y = d_{\lambda,m}(y)$, their *intrinsic co-leaf product* $x \odot_{\lambda,m} y \in \mathcal{L}_{g,\lambda}$ is defined by replacing the global scalars in the foliated product $\otimes_{\lambda,m}$ with the intrinsic leaf depths:

$$x \odot_{\lambda,m} y \equiv \nabla_{\lambda,m}\Big(x,\ d_x(d_y - 1)\Big) = \big(g,\ d_x \cdot d_y\big)_\lambda. \tag{3.34}$$

Iterating Equation (3.34) $\alpha \geq 1$ times for a leaf element $q = (g,p)_\lambda \in \mathcal{L}_{g,\lambda}$ defines the *intrinsic co-leaf power* $q^{\odot\alpha} \equiv \nabla_{\lambda,m}(q,\ p^\alpha - p) = (g,\ p^\alpha)_\lambda$, with $q^{\odot 0} \equiv (g,1)_\lambda$.

Theorem 3.20 (Leaf-Local Fundamental Theorem of Arithmetic)**.** *For every foliation degree $m \geq 1$, direction $\lambda \in \{0, \frac{1}{2}, 1\}$, and generator g, the positive-depth sub-leaf $\mathcal{L}^*_{g,\lambda} = \{(g,d)_\lambda : d \geq 1\}$ equipped with $\odot_{\lambda,m}$ is a commutative monoid with multiplicative identity $u_{g,\lambda} = (g,1)_\lambda \in S_{k_0+1,m}$ and unique factorization into local leaf-depth primes $\mathcal{D}_{g,\lambda,m} = \mathcal{L}_{g,\lambda} \cap \mathcal{D}_{\lambda,m}$. Specifically, every element $x \in \mathcal{L}_{g,\lambda} \setminus \{z_{g,\lambda}, u_{g,\lambda}\}$ ($d_{\lambda,m}(x) \geq 2$) admits a canonical decomposition*

$$x = q_1^{\odot\alpha_1} \odot_{\lambda,m} q_2^{\odot\alpha_2} \odot_{\lambda,m} \cdots \odot_{\lambda,m} q_\ell^{\odot\alpha_\ell} = \nabla_{\lambda,m}\left(z_{g,\lambda},\ \prod_{i=1}^{\ell} \big(d_{\lambda,m}(q_i)\big)^{\alpha_i}\right), \tag{3.35}$$

where $q_1 < q_2 < \cdots < q_\ell$ are distinct leaf-depth primes in $\mathcal{D}_{g,\lambda,m}$, $\alpha_i \in \mathbb{N}^*$, and $z_{g,\lambda} = (g,0)_\lambda \in S_{k_0,m}$ is the leaf root. This decomposition is unique up to the ordering of the factors.

Proof. For fixed (g,λ,m), the local depth map $d_{\lambda,m} : \mathcal{L}^*_{g,\lambda} \to \mathbb{N}^*$ given by $(g,d)_\lambda \mapsto d = k_x - k_0$ is a strictly monotonic bijection with inverse $d \mapsto \nabla_{\lambda,m}(z_{g,\lambda},\ d)$. By Equation (3.34) and the longitudinal step-additivity of the transport operator $\nabla_{\lambda,m}$, we have

$$d_{\lambda,m}(x \odot_{\lambda,m} y) = d_x + d_x(d_y - 1) = d_x d_y = d_{\lambda,m}(x) \cdot d_{\lambda,m}(y).$$

Consequently, $d_{\lambda,m} : (\mathcal{L}^*_{g,\lambda}, \odot_{\lambda,m}) \xrightarrow{\sim} (\mathbb{N}^*, \cdot)$ is a monoid isomorphism mapping the leaf-unit $u_{g,\lambda} = (g,1)_\lambda$ to 1 and the leaf-depth primes $\mathcal{D}_{g,\lambda,m} = \{(g,p)_\lambda : p \in \mathbb{P}\}$ bijectively onto the classical primes $\mathbb{P}$. Pulling the classical Fundamental Theorem of Arithmetic on $(\mathbb{N}^*, \cdot)$ back along $d^{-1}_{\lambda,m}$ yields the unique canonical decomposition (3.35). At the flat Peano limit $m = 1$, where $g = 0$, $k_0 = 0$, and $d_{\lambda,1}(x) = x$, Equation (3.35) reduces identically to the classical Fundamental Theorem of Arithmetic $x = \prod_{i=1}^{\ell} p_i^{\alpha_i}$. □

Because every integer $x \in S_{k,m}$ sits at the simultaneous transverse intersection of three directional leaves $L_{g_l,0} \cap V_{g_v,1/2} \cap R_{g_r,1}$, Theorem 3.20 endows each integer with a triad of leaf-local prime factorizations governed by its local depth vector $\mathbf{d}_m(x) = \big(d_{0,m}(x),\ d_{1/2,m}(x),\ d_{1,m}(x)\big)$. In the quadratic foliation $\mathbb{N}_2$, these three directional depths obey an exact cross-directional duality.

Corollary 3.21 (Triadic Depth-Coupling and Minimal Triple Leaf-Depth Prime in $\mathbb{N}_2$)**.** *In the quadratic foliation $\mathbb{N}_2$ ($m = 2$), every integer $x = k^2 + r \in S_{k,2}$ ($0 \leq r \leq 2k$) has boundary generators $g_l(x) = r$ and $g_r(x) = 2k - r$ with birth shells $k_0(g,\lambda,2) = \lceil g/2 \rceil$ ($\lambda \in \{0,1\}$), and vertical generator $g_v(x) = r - k$ with birth shell $k_0(g_v, \frac{1}{2}, 2) = |r - k|$. Its local depth triad $\mathbf{d}_2(x) = \big(d_{0,2}(x),\ d_{1/2,2}(x),\ d_{1,2}(x)\big)$ is given in closed form by the cross-generator relations:*

$$d_{0,2}(x) = \left\lfloor \frac{g_r(x)}{2} \right\rfloor, \qquad d_{1/2,2}(x) = \min\big(g_l(x),\ g_r(x)\big), \qquad d_{1,2}(x) = \left\lfloor \frac{g_l(x)}{2} \right\rfloor, \tag{3.36}$$

which satisfy the exact triadic coupling identities:

$$d_{0,2}(x) + d_{1,2}(x) = \begin{cases} k & \text{if } r \text{ is even,} \\ k-1 & \text{if } r \text{ is odd,} \end{cases} \qquad \text{and} \qquad \min\big(d_{0,2}(x),\ d_{1,2}(x)\big) = \left\lfloor \frac{d_{1/2,2}(x)}{2} \right\rfloor. \tag{3.37}$$

In particular:

1. ***Goldbach Pairing of Boundary Leaf-Depth Primes:*** *An integer $x \in S_{k,2}$ is simultaneously a Left and Right leaf-depth prime ($x \in \mathcal{D}_{0,2} \cap \mathcal{D}_{1,2}$) if and only if $\big(d_{0,2}(x),\, d_{1,2}(x)\big)$ forms a two-prime Goldbach partition of k (for r even) or $k-1$ (for r odd).*

2. ***Exclusion of*** $(2,2,2)$ ***and Minimal Triple Leaf-Depth Prime:*** *By the second identity in Equation (3.37), any triple leaf-depth prime $x \in \mathcal{D}_{*,2} = \mathcal{D}_{0,2} \cap \mathcal{D}_{1/2,2} \cap \mathcal{D}_{1,2}$ requires $\lfloor d_{1/2,2}(x)/2 \rfloor \geq 2$, which forces $d_{1/2,2}(x) \geq 5$ and rules out $\mathbf{d}_2(x) = (2,2,2)$. The minimal triple leaf-depth prime in $\mathbb{N}_2$ is the central spine integer $x = 30 \in S_{5,2}$ ($k = 5, r = 5$), which achieves $\mathbf{d}_2(30) = (2,5,2) \in \mathbb{P}^3$.*

Proof. For $x = k^2 + r \in S_{k,2}$, the shell capacity condition $g < |S_{\kappa,2}| = 2\kappa + 1$ yields $k_0(g, \lambda, 2) = \lceil g/2 \rceil$ for $\lambda \in \{0, 1\}$. Thus $d_{0,2}(x) = k - \lceil r/2 \rceil = \lfloor (2k - r)/2 \rfloor = \lfloor g_r(x)/2 \rfloor$ and $d_{1,2}(x) = k - \lceil (2k-r)/2 \rceil = \lfloor r/2 \rfloor = \lfloor g_l(x)/2 \rfloor$. Along $\lambda = \frac{1}{2}$, the condition $|g_v(x)| \leq \kappa$ gives $k_0(g_v, \frac{1}{2}, 2) = |r - k|$, so $d_{1/2,2}(x) = k - |r-k| = \min(r, 2k-r) = \min(g_l(x), g_r(x))$. Taking the minimum of $d_{0,2}(x)$ and $d_{1,2}(x)$ immediately gives $\min(d_{0,2}(x), d_{1,2}(x)) = \lfloor \min(g_l(x), g_r(x))/2 \rfloor = \lfloor d_{1/2,2}(x)/2 \rfloor$. For all three depths to be prime, $\min(d_{0,2}(x), d_{1,2}(x)) \geq 2 \implies d_{1/2,2}(x) \geq 4$, and since $d_{1/2,2}(x) \in \mathbb{P}$, the minimal vertical depth is $d_{1/2,2}(x) = 5$, realized minimally at $g_l = g_r = 5$ ($k = 5, r = 5, x = 30$) with $\mathbf{d}_2(30) = (2,5,2)$. □

Example 3.6 (Multi-Foliation Prime Factorizations of the Single Scalar $x = 861$)**.** To illustrate how a single scalar integer simultaneously admits multiple distinct canonical prime factorizations across different foliations and directions, consider the 3-digit interior integer $x = 861$. In the flat Peano foliation $\mathbb{N}_1$ ($m = 1$), its classical prime decomposition is $861 = 3 \times 7 \times 41$. In the quadratic foliation $\mathbb{N}_2$ ($m = 2$) and the cubic foliation $\mathbb{N}_3$ ($m = 3$), its partitioned coordinate matrices are:

$$M_{861,2} = \left[\begin{array}{c|ccc} 29 & 20 & -9 & 38 \\ 20 & 19 & 20 & 10 \end{array}\right], \qquad M_{861,3} = \left[\begin{array}{c|ccc} 9 & 132 & -3 & 138 \\ 132 & 2 & 8 & 2 \end{array}\right],$$

where the first column records the global shell coordinates $[k, r]^\top$ ($x = k^m + r$) and the remaining three columns display the directional leaf coordinates $[g_\lambda, d_\lambda]^\top \equiv (g, d)_\lambda$ for $\lambda \in \{0, \frac{1}{2}, 1\}$, with corresponding birth shells $k_0(g_\lambda) = k - d_\lambda$:

- **In $\mathbb{N}_2$ ($k = 29$, $r = 20$):** Reading columns 2–4 of $M_{861,2}$ vertically yields the triad of leaf coordinates $(20, 19)_0$, $(-9, 20)_{1/2}$, and $(38, 10)_1$ with birth shells $\mathbf{k}_{0,2}(861) = (10,\ 9,\ 19)$. Because the local depths factor as $\mathbf{d}_2(861) = (19,\ 2^2 \times 5,\ 2 \times 5)$, the scalar 861 is a Left leaf-depth prime $(20, 19)_0$, while decomposing along the Vertical leaf $V_{-9,2}$ into $(-9, 2)_{1/2}^{\odot 2} \odot_{1/2,2} (-9, 5)_{1/2} = 123^{\odot 2} \odot_{1/2,2} 201$ and along the Right leaf $R_{38,2}$ into $(38, 2)_1 \odot_{1,2} (38, 5)_1 = 445 \odot_{1,2} 586$.

- **In $\mathbb{N}_3$ ($k = 9$, $r = 132$):** Reading columns 2–4 of $M_{861,3}$ vertically yields the triad of leaf coordinates $(132, 2)_0$, $(-3, 8)_{1/2}$, and $(138, 2)_1$ with birth shells $\mathbf{k}_{0,3}(861) = (7,\ 1,\ 7)$. Because $\mathbf{d}_3(861) = (2,\ 2^3,\ 2)$, the scalar 861 is simultaneously a Left and Right leaf-depth prime while decomposing along the Vertical leaf $V_{-3,3}$ as the exact intrinsic leaf-cube $(-3, 2)_{1/2}^{\odot 3} = 42^{\odot 3}$.

Table 5 contrasts these canonical prime factorizations for the single scalar $x = 861$.

4 Discrete Holonomy and Arithmetic Holography in $\mathbb{N}_2$

4.1 Shell-to-Leaf Holographic Encoding

We begin by establishing how classical multiplication by a leaf successor induces directed translation along the leaves of $\mathbb{N}_2$.

Table 5: Canonical prime factorizations of the single scalar $x = 861$ across the classical Peano regime ($m = 1$), the quadratic foliation ($m = 2$), and the cubic foliation ($m = 3$).

Foliation Regime	**Direction** λ	**Depth Factorization** $d_{\lambda,m}(861)$	**Canonical Prime Factorization of the Scalar** $x = 861$
Classical ($\mathbb{N}_1$)	All λ	$861 = 3 \times 7 \times 41$	$861 = 3 \times 7 \times 41$
Quadratic ($\mathbb{N}_2$)	Left ($\lambda = 0$)	$19 \in \mathbb{P}$	$861 = 861^{\odot 1}$ (Leaf-Depth Prime)
	Vertical ($\lambda = \frac{1}{2}$)	$20 = 2^2 \times 5$	$861 = 123^{\odot 2} \odot_{1/2,2} 201$
	Right ($\lambda = 1$)	$10 = 2 \times 5$	$861 = 445 \odot_{1,2} 586$
Cubic ($\mathbb{N}_3$)	Left ($\lambda = 0$)	$2 \in \mathbb{P}$	$861 = 861^{\odot 1}$ (Leaf-Depth Prime)
	Vertical ($\lambda = \frac{1}{2}$)	$8 = 2^3$	$861 = 42^{\odot 3}$
	Right ($\lambda = 1$)	$2 \in \mathbb{P}$	$861 = 861^{\odot 1}$ (Leaf-Depth Prime)

Proposition 4.1 (Six-Branch Multiplicative Leaf Identities)**.** *For any $g, d \in \mathbb{N}$, the following polynomial identities hold across the six leaf parameterizations of $\mathbb{N}_2$:*

$$\big[(g+d)^2 + d\big]\big[(g+d+1)^2 + d + 1\big] = \big[g + (g+d)^2 + 2d\big]^2 + (g+d)^2 + 2d \tag{4.1}$$

$$\big[(g+d)^2 + d + 2g\big]\big[(g+d+1)^2 + d + 1 + 2g\big] = \big[g + (g+d)^2 + 2d + 2g\big]^2 + \big[(g+d)^2 + 2d + 2g\big] + 2g \tag{4.2}$$

$$\big[(g+d)^2 + 2d\big]\big[(g+d+1)^2 + 2(d+1)\big] = \big[g + (g+d)^2 + 3d\big]^2 + 2\big[(g+d)^2 + 3d\big] \tag{4.3}$$

$$\big[(g+d)^2 + 2d - 1\big]\big[(g+d+1)^2 + 2(d+1) - 1\big] = \big[g + (g+d)^2 + 3d - 1\big]^2 + 2\big[(g+d)^2 + 3d - 1\big] - 1 \tag{4.4}$$

$$\big[(g+d)^2 + 2g\big]\big[(g+d+1)^2 + 2g\big] = \big[g + (g+d)^2 + 2g + d\big]^2 + 2g \tag{4.5}$$

$$\big[(g+d)^2 + 2g + 1\big]\big[(g+d+1)^2 + 2g + 1\big] = \big[g + (g+d)^2 + 2g + d + 1\big]^2 + 2g + 1 \tag{4.6}$$

Proof. Immediate by expanding both sides in $\mathbb{Z}[g, d]$. □

Geometrically, Equations (4.1)–(4.6) encode the exact algebraic leaf-invariance of consecutive scalar products across the six parity-split directional families of the quadratic foliation $\mathbb{N}_2$:

- **Vertical Leaves ($\lambda = \frac{1}{2}$):** Equation (4.1) parameterizes the negative vertical leaf $V_{-g}(d) = (g+d)^2 + d$, while Equation (4.2) parameterizes the positive vertical leaf $V_{+g}(d) = (g+d)^2 + d + 2g$.
- **Right Leaves ($\lambda = 1$):** Equation (4.3) parameterizes the even-indexed right leaf $R_{2g}(d) = (g+d)^2 + 2d$, while Equation (4.4) parameterizes the odd-indexed right leaf $R_{2g+1}(d) = (g+d)^2 + 2d - 1$ ($d \geq 1$).

- **Left Leaves ($\lambda = 0$):** Equation (4.5) parameterizes the even-indexed left leaf $L_{2g}(d) = (g+d)^2 + 2g$, while Equation (4.6) parameterizes the odd-indexed left leaf $L_{2g+1}(d) = (g+d)^2 + (2g+1)$ $(d \geq 1)$.

In each of the six branches, multiplying an integer at local depth d by its immediate longitudinal successor at depth $d+1$ along the same leaf does not scatter the result across the foliation; instead, the product lands identically back on the *exact same leaf* at a quadratically compounded local depth $D = (g+d)^2 + \alpha d + \beta g$. This structural closure of consecutive leaf-elements under classical scalar multiplication motivates the following general theorem.

Theorem 4.2 (The Universal Equation of Translation)**.** *For any direction $\lambda \in \{0, \frac{1}{2}, 1\}$ and leaf coordinate pair $n = (g,d)_\lambda \in \mathbb{N}_2$, multiplying n by its immediate leaf successor $(g, d+1)_\lambda = \nabla_\lambda(n, 1)$ preserves g and translates the local depth d forward by n:*

$$(g,d)_\lambda \cdot (g,d+1)_\lambda = \big(g,\ d + (g,d)_\lambda\big)_\lambda = \nabla_\lambda(n,n). \tag{4.7}$$

Proof. Let $k = \lfloor \sqrt{n} \rfloor$. By Equation (2.12), $(g, d+1)_\lambda = \nabla_\lambda(n,1) = n + 2k + 1 + 2\lambda$. Multiplying by n gives $n\nabla_\lambda(n,1) = n^2 + 2nk + n + 2\lambda n = \nabla_\lambda(n,n) = (g, d+n)_\lambda$. □

Definition 4.3 (Holographic Translation Operator $\widehat{T}_\lambda$)**.** For any $\lambda \in \{0, \frac{1}{2}, 1\}$ and $n \in \mathbb{N}^*$, the holographic translation (self-shift) operator $\widehat{T}_\lambda : \mathbb{N}^* \to \mathbb{N}^*$ is defined by:

$$\widehat{T}_\lambda(n) \equiv n \cdot \nabla_\lambda(n,1) = \nabla_\lambda(n,n). \tag{4.8}$$

For $n = k^2 + r$ $(0 \leq r \leq 2k)$, $\widehat{T}_\lambda(n) = (k+n)^2 + (r + 2\lambda n)$ satisfies $0 \leq r + 2\lambda n \leq 2(k+n)$, so $\widehat{T}_\lambda(n)$ always resides in shell $K = \lfloor \sqrt{\widehat{T}_\lambda(n)} \rfloor = k + n$.

Applying $\widehat{T}_\lambda$ across a horizontal shell S_k maps the entire shell injectively onto a single 1D leaf (Figure 4):

$$\lambda = 0: \quad \underbrace{\widehat{T}_0(N)}_{\in V_{-(k^2+k)}} = \underbrace{N}_{\in S_k} \times \underbrace{\nabla_0(N,1)}_{\in S_{k+1}} = \nabla_0(N,N), \tag{4.9}$$

$$\lambda = \frac{1}{2}: \quad \underbrace{\widehat{T}_{1/2}(N)}_{\in R_{k^2+2k}} = \underbrace{N}_{\in S_k} \times \underbrace{\nabla_{1/2}(N,1)}_{\in S_{k+1}} = \nabla_{1/2}(N,N). \tag{4.10}$$

Theorem 4.4 (Bijective Shell-to-Leaf Encoding)**.** *The mappings $\widehat{T}_0 : S_k \to V_{-(k^2+k)}$ and $\widehat{T}_{1/2} : S_k \to R_{k^2+2k}$ are injective, and the constituent factors in S_k and S_{k+1} are uniquely recoverable from the 1D leaf coordinates of the product.*

Proof. For $N = k^2 + r \in S_k$ $(0 \leq r \leq 2k)$, $\widehat{T}_0(N) = \big((k+1)^2 + r\big)(k^2 + r) = (k^2 + k + r)^2 + r$ has target shell $K = k^2 + k + r$ and residue $r_K = r$, yielding constant vertical generator $g_v = r_K - K = -(k^2 + k)$ and recovering $r = r_K$ and $k^2 + k = K - r_K$. Similarly, $\widehat{T}_{1/2}(N) = \big((k+1)^2 + r + 1\big)(k^2 + r) = (k^2 + k + r)^2 + k^2 + 2r$ resides in shell $K = k^2 + k + r$ with residue $r_K = k^2 + 2r$, yielding constant right generator $g_r = 2K - r_K = k^2 + 2k$ (so $\widehat{T}_{1/2}(S_k) \subset R_{k^2+2k}$) from which (k, r) are uniquely determined. □

4.2 Discrete Holonomy and Curvature on $\mathbb{N}_2$ and $\mathbb{Z}_2$

Whereas the affine transport operator $\nabla_\lambda(n,s)$ shifts an integer by an external step parameter s, the self-shift operator $\widehat{T}_\lambda(n) = \nabla_\lambda(n,n)$ couples the step count directly to the integer n itself. We quantify the discrete holonomy and curvature of the lattice by evaluating the commutator of $\widehat{T}_\lambda$ across distinct directions $\lambda_1 \neq \lambda_2 \in \{0, \frac{1}{2}, 1\}$.

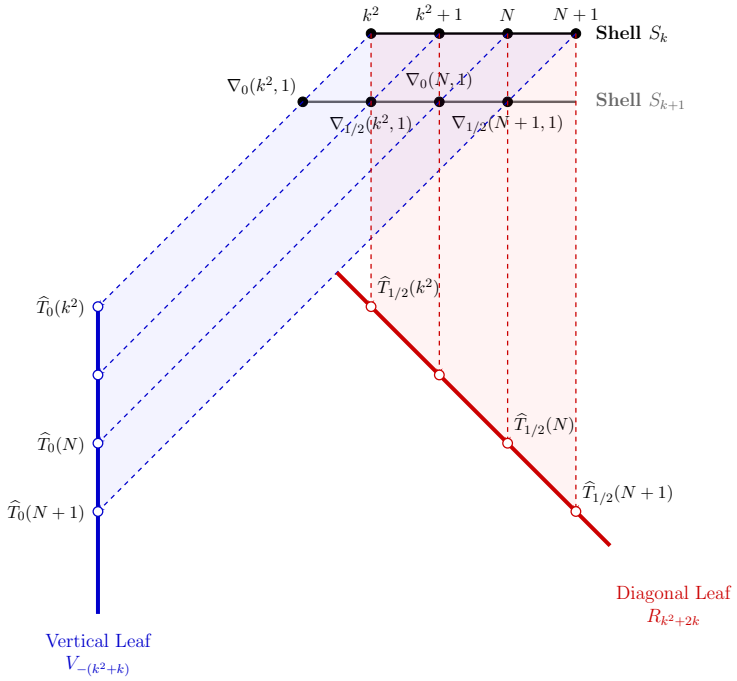


Figure 4: Shell-to-leaf projection via $\widehat{T}_0$ and $\widehat{T}_{1/2}$. Elements $N = k^2+r \in S_k$ are mapped through S_{k+1} onto the single vertical leaf $V_{-(k^2+k)}$ (blue) or the single right-diagonal leaf R_{k^2+2k} (red).

Theorem 4.5 (Non-Commutativity of Holographic Translation)**.** *For any $n \in \mathbb{N}^*$ and distinct directions $\lambda_1, \lambda_2 \in \{0, \frac{1}{2}, 1\}$ $(\lambda_1 \neq \lambda_2)$, sequential applications of $\widehat{T}_{\lambda_1}$ and $\widehat{T}_{\lambda_2}$ satisfy:*

$$\begin{aligned}\big[\widehat{T}_{\lambda_1}, \widehat{T}_{\lambda_2}\big](n) &= \widehat{T}_{\lambda_1}\big(\widehat{T}_{\lambda_2}(n)\big) - \widehat{T}_{\lambda_2}\big(\widehat{T}_{\lambda_1}(n)\big) \\ &= 2(\lambda_2 - \lambda_1)\Big[(2n-1)A(n) + n\big(2n(\lambda_1+\lambda_2) + 2k + 2n + 1\big)\Big] \neq 0,\end{aligned} \tag{4.11}$$

where $k = \lfloor \sqrt{n} \rfloor$ and $A(n) = n^2 + 2nk + n$.

Proof. Write $\widehat{T}_\lambda(n) = A(n) + 2\lambda n$. Let $M = \widehat{T}_{\lambda_2}(n)$ and $N = \widehat{T}_{\lambda_1}(n)$, both residing in shell $K = k+n$. Evaluating $\widehat{T}_{\lambda_1}(M) - \widehat{T}_{\lambda_2}(N) = (M^2 - N^2) + (2k+2n+1)(M-N) + 2(\lambda_1 M - \lambda_2 N)$ and substituting $M - N = 2n(\lambda_2 - \lambda_1)$, $M + N = 2A(n) + 2n(\lambda_1 + \lambda_2)$, and $2(\lambda_1 M - \lambda_2 N) = -2A(n)(\lambda_2 - \lambda_1)$ yields the stated expression, which is non-zero for all $n \geq 1$ and $\lambda_1 \neq \lambda_2$. □

Corollary 4.6 (Discrete Curvature of $\mathbb{N}_2$)**.** *The Chebyshev distance*

$$\mathcal{R}_{\lambda_1,\lambda_2}(n) = \delta\big(\widehat{T}_{\lambda_1}(\widehat{T}_{\lambda_2}(n)),\, \widehat{T}_{\lambda_2}(\widehat{T}_{\lambda_1}(n))\big)$$

between the two two-step endpoints generated by $\widehat{T}_{\lambda_1}$ and $\widehat{T}_{\lambda_2}$ is:

$$\mathcal{R}_{\lambda_1,\lambda_2}(n) = 2A(n)|\lambda_1 - \lambda_2|, \qquad A(n) = n^2 + 2n\lfloor\sqrt{n}\rfloor + n. \tag{4.12}$$

Proof. The terminal shell indices are $K_1 = k+n+M$ and $K_2 = k+n+N$, giving $\Delta k = |M-N| = 2n|\lambda_2 - \lambda_1|$. The vertical generators $g_i = r_i - K_i$ differ by $|\Delta g| = 2|\lambda_1 M - \lambda_2 N| = 2A(n)|\lambda_1 - \lambda_2|$. Since $A(n) > n$ for $n \geq 1$, $\max(\Delta k, |\Delta g|) = 2A(n)|\lambda_1 - \lambda_2|$. □

Remark 4.7 (Forbidden Shells in the Self-Shift Image)**.** Because $\widehat{T}_\lambda(n)$ maps $n \in S_k$ to shell $K(n) = n + k$, passing from $n = k^2 + 2k \in S_k$ $(K = k^2 + 3k)$ to $n' = (k+1)^2 \in S_{k+1}$ $(K = k^2 + 3k + 2)$ skips the shell S_{k^2+3k+1} $(S_5, S_{11}, S_{19}, S_{29}, \dots)$ for every $k \geq 1$.

Extending $\widehat{T}_\lambda$ to all $z \in \mathbb{Z}_2$ via $\widehat{T}_\lambda(z) \equiv \widehat{\nabla}_\lambda(z,z) = \operatorname{sgn}(z)\nabla_\lambda(|z|,|z|)$ (and defining the reverse zero-projection $\widehat{T}^*_\lambda(z) \equiv \widehat{\nabla}_\lambda(z,-z) = z \otimes_{\lambda,2} 0 = -\widehat{T}_\lambda(z)$ for $|z| \geq 2$) yields:

Theorem 4.8 (Global and Normalized Curvature on $\mathbb{Z}_2$)**.** *For all $z \in \mathbb{Z}$ and $\lambda_1 \neq \lambda_2 \in \{0, \frac{1}{2}, 1\}$:*

1. ***Parity and Double-Bounce Invariance:*** *For $|z| \geq 2$,*

$$[\widehat{T}_{\lambda_1}, \widehat{T}_{\lambda_2}](-z) = -[\widehat{T}_{\lambda_1}, \widehat{T}_{\lambda_2}](z), \qquad [\widehat{T}^*_{\lambda_1}, \widehat{T}^*_{\lambda_2}](z) = [\widehat{T}_{\lambda_1}, \widehat{T}_{\lambda_2}](z),$$
$$\mathcal{R}_{\lambda_1,\lambda_2}(z) = 2A(|z|)|\lambda_1 - \lambda_2| \geq 0.$$

2. ***Asymptotic Constant Limit:*** *The normalized curvature $\widetilde{\mathcal{R}}_{\lambda_1,\lambda_2}(z) \equiv z^{-2}\mathcal{R}_{\lambda_1,\lambda_2}(z)$ satisfies $\widetilde{\mathcal{R}}_{\lambda_1,\lambda_2}(\pm 1) = 8|\lambda_1 - \lambda_2|$ and converges at infinity to:*

$$\lim_{|z|\to\infty} \widetilde{\mathcal{R}}_{\lambda_1,\lambda_2}(z) = \lim_{|z|\to\infty} 2\left(1 + \frac{2\lfloor\sqrt{|z|}\rfloor}{|z|} + \frac{1}{|z|}\right)|\lambda_1 - \lambda_2| = 2|\lambda_1 - \lambda_2|. \tag{4.13}$$

Proof. Part (1) follows from $\widehat{T}_\lambda(-z) = -\widehat{T}_\lambda(z)$ and $\widehat{T}^*_\lambda(z) = -\widehat{T}_\lambda(z)$. Part (2) follows from the squeeze bounds $\frac{1}{\sqrt{|z|}} - \frac{1}{|z|} < \frac{\lfloor\sqrt{|z|}\rfloor}{|z|} \leq \frac{1}{\sqrt{|z|}}$ as $|z| \to \infty$. □

4.3 Conical Embedding of the Quadratic Foliation $\mathbb{Z}_2$

Embedding the planar triangular lattice $\mathbb{N}_2$ (and its reflected completion $\mathbb{Z}_2$) onto a three-dimensional cone wraps each horizontal shell S_k into a closed circular ring while mapping the vertical leaves V_g to longitudinal meridians and the diagonal leaves L_g, R_g to counter-winding helices.

Definition 4.9 (Conical Embedding Map $\widehat{\Phi}$)**.** For any $z \in \mathbb{Z}_2^*$ with $k = \lfloor\sqrt{|z|}\rfloor$ and $g_v = |z| - k^2 - k \in [-k, k]$, the conical embedding $\widehat{\Phi} : \mathbb{Z}_2 \to \mathbb{R}^3$ is defined by $\widehat{\Phi}(0) = (0, 0, 0)^T$ and:

$$\widehat{\Phi}(z) = \begin{pmatrix} Wk\cos\left(\pi\dfrac{g_v}{k}\right) \\ Wk\sin\left(\pi\dfrac{g_v}{k}\right) \\ -\operatorname{sgn}(z)Dk \end{pmatrix}, \qquad D = W\sqrt{\pi^2 - 1}, \tag{4.14}$$

where $D = W\sqrt{\pi^2 - 1}$ equates the unit circumferential arc step $\Delta s_\theta = \pi W$ to the longitudinal slant step $\Delta s_k = \sqrt{W^2 + D^2}$.

Theorem 4.10 (Boundary Identification Along the Conical Seam)**.** *Under $\widehat{\Phi}$, the left boundary ($g_v = -k$, $|z| = k^2$) and right boundary ($g_v = +k$, $|z| = k^2 + 2k$) of each shell S_k coincide along the ray $\big(-Wk,\, 0,\, -\operatorname{sgn}(z)Dk\big)^T$, inducing the identification $k^2 \equiv_{\widehat{\Phi}} k^2 + 2k$ and closing each shell S_k into a circle (Figure 5).*

Proof. Immediate from $\cos(-\pi) = \cos(\pi) = -1$ and $\sin(-\pi) = \sin(\pi) = 0$ in Equation (4.14). □

4.4 The Arithmetic Holographic Conjecture: Prime Packets and Sieve Coupling

4.4.1 From Pointwise Prime Gaps to Shell Prime Packets

Classical analytic number theory investigates the distribution of prime numbers ($\mathbb{P} = \{2, 3, 5, 7, \dots\}$) along the 1D line ($m = 1$), where individual prime gaps $p_{i+1} - p_i$ oscillate between remaining infinitely often bounded ($\liminf_{i\to\infty}(p_{i+1} - p_i) \leq 246$) [10, 11, 12] and growing arbitrarily large ($\limsup_{i\to\infty}(p_{i+1} - p_i) = \infty$) [13, 14].

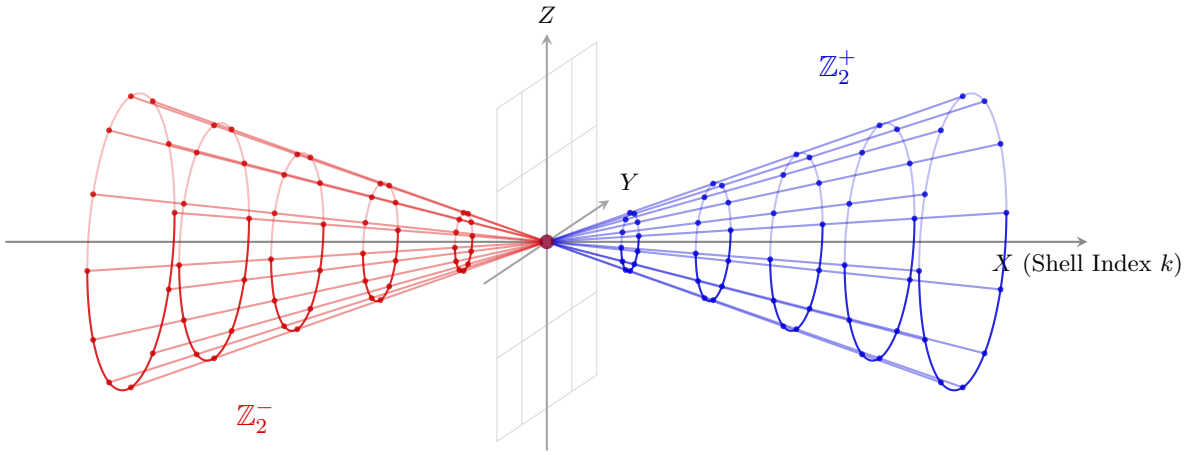


Figure 5: Conical embedding of the reflected quadratic foliation $\mathbb{Z}_2$, joining the negative half-lattice $\mathbb{Z}_2^-$ and positive half-lattice $\mathbb{Z}_2^+$ at the origin 0: a native discrete metrizable space equipped with multi-valued non-commutative arithmetic, discrete holonomy, and curvature.

Within the quadratic foliation $\mathbb{N}_2$, the natural unit of scale is the circular shell $S_n = \{n^2, n^2+1, \ldots, (n+1)^2-1\}$ at shell index $k = n$. Accordingly, we group the classical primes within S_n into a **Prime Packet**:

$$\mathcal{P}(S_n) \equiv \mathbb{P} \cap S_n = \big\{p \in \mathbb{P} \;\big|\; n^2 \le p < (n+1)^2\big\}, \qquad \big|\mathcal{P}(S_n)\big| = \pi\big((n+1)^2\big) - \pi(n^2). \tag{4.15}$$

By the Eratosthenes sieve, an integer $x \in S_n$ ($n^2 \le x < (n+1)^2$) is prime if and only if it is not divisible by any prime $p \le \lfloor\sqrt{x}\rfloor = n$. Thus, the prime packet $\mathcal{P}(S_n)$ at shell index $k = n$ is completely determined by the primes residing in the initial interval $[1, n]$ (which terminates at shell index $k = \lfloor\sqrt{n}\rfloor$), whereas the intermediate primes in (n, n^2) exert no sieve constraint on S_n.

4.4.2 Exact Holographic Conservation of Local Prime-Depth Elements

Before stating the asymptotic conjecture for $\mathcal{P}(S_n)$, we prove that for the **Local Prime-Depth Elements** $\mathcal{D}_{\lambda,2}$ (Definition 3.16, where $\nabla_\lambda\big(a, (x-1)\cdot d_\lambda(a)\big) = p$ has no solution), the count on shell S_n is given deterministically by $\pi(n)$ across all three directions.

Theorem 4.11 (Exact Holographic Conservation of Local Prime-Depth Elements)**.** *For every shell index $n \in \mathbb{N}^*$ and direction $\lambda \in \{0, \frac{1}{2}, 1\}$, the cardinality of $\mathcal{D}_{\lambda,2} \cap S_n$ is invariant across λ and equals:*

$$\big|\mathcal{D}_{0,2} \cap S_n\big| = \big|\mathcal{D}_{1/2,2} \cap S_n\big| = \big|\mathcal{D}_{1,2} \cap S_n\big| = \pi(n) + \pi(n-1) = \begin{cases} 2\pi(n) & \text{if } n \notin \mathbb{P}, \\ 2\pi(n) - 1 & \text{if } n \in \mathbb{P}. \end{cases} \tag{4.16}$$

Moreover, on each half-shell $S_n^+ = \{n^2 + r \mid n \le r \le 2n\}$ and $S_n^- = \{n^2 + r \mid 0 \le r \le n\}$ along $\lambda = \frac{1}{2}$:

$$\big|\mathcal{D}_{1/2,2} \cap S_n^+\big| = \big|\mathcal{D}_{1/2,2} \cap S_n^-\big| = \pi(n). \tag{4.17}$$

Proof. By Proposition 3.17, $x \in \mathcal{D}_{\lambda,2} \iff d_{\lambda,2}(x) \in \mathbb{P}$. For $x = n^2 + r \in S_n$ ($0 \le r \le 2n$):

1. **On $\lambda = 1$:** $d_1(x) = \lfloor r/2 \rfloor$ attains each integer $d \in \{0, \ldots, n-1\}$ twice ($r = 2d, 2d+1$) and $d = n$ once ($r = 2n$), giving $2\pi(n-1) + \mathbb{I}_{\mathbb{P}}(n) = \pi(n) + \pi(n-1)$.
2. **On $\lambda = 0$:** $d_0(x) = n - \lceil r/2 \rceil = \lfloor (2n-r)/2 \rfloor$ is the reflection $r \mapsto 2n - r$ of $d_1(x)$, yielding $\pi(n) + \pi(n-1)$.

3. **On $\lambda = \frac{1}{2}$:** $d_{1/2}(x) = n - |r - n|$ sweeps $\{0, 1, \ldots, n\}$ bijectively on S_n^- and $\{n, \ldots, 0\}$ bijectively on S_n^+, giving $\pi(n)$ on each half-shell and $\pi(n) + \pi(n-1)$ on S_n.

□

4.4.3 The Arithmetic Holographic Conjecture and the $m = 2$ Riemann Hypothesis Bound

By Theorem 4.11, each prime $p \le n$ in $[1, n]$ corresponds to a consecutive pair $\{n^2 + 2p,\ n^2 + 2p + 1\}$ in $\mathcal{D}_{1,2} \cap S_n$. Because the two elements of each consecutive pair have opposite parities, one is always even, leaving half of the $2\pi(n)$ elements as odd prime candidates. Analytically, the Prime Number Theorem density near n^2 is $\rho_{\text{prime}}(n^2) \sim \frac{1}{\ln(n^2)} = \frac{1}{2\ln n}$, while $|S_n| = 2n+1 \sim 2n$, so the factor of 2 cancels:

$$\big|\mathcal{P}(S_n)\big| \approx |S_n| \cdot \rho_{\text{prime}}(n^2) \sim (2n) \cdot \frac{1}{2\ln n} = \frac{n}{\ln n} \sim \pi(n). \tag{4.18}$$

Conjecture 4.12 (Arithmetic Holographic Conjecture and Square-Root Deviation Bound)**.** Let $\mathcal{P}(S_n) = S_n \cap \mathbb{P}$ denote the set of classical primes residing in the n-th horizontal shell $S_n = \{n^2, \ldots, (n+1)^2 - 1\}$ of the quadratic foliation $\mathbb{N}_2$, and let $\pi(n) = \big|\{p \in \mathbb{P} : p \le n\}\big|$ denote the cumulative prime counting function up to the shell index n. Then:

1. **Strict Local Positivity (Legendre–Oppermann Shell Occupation):** Every horizontal shell S_n $(n \ge 1)$ contains at least two prime numbers:

$$\big|\mathcal{P}(S_n)\big| = \pi\big((n+1)^2 - 1\big) - \pi(n^2) \ge 2 \qquad (\forall\, n \ge 1). \tag{4.19}$$

2. **Bulk–Boundary Asymptotic Equipartition:** As $n \to \infty$, the prime population of the single n-th horizontal shell S_n is asymptotically equal to the cumulative prime count from 1 to n:

$$\lim_{n\to\infty} \frac{\big|\mathcal{P}(S_n)\big|}{\pi(n)} = 1, \qquad \text{with common leading density } \big|\mathcal{P}(S_n)\big| \sim \pi(n) \sim \frac{n}{\ln n}. \tag{4.20}$$

3. **Strict Square-Root Holographic Envelope:** For all shell indices $n \ge 2$, the absolute deviation of the shell prime count $\big|\mathcal{P}(S_n)\big|$ from the leading holographic density $\frac{n}{\ln n}$ is strictly bounded by the square root of the shell index:

$$\Big|\big|\mathcal{P}(S_n)\big| - \frac{n}{\ln n}\Big| < n^{1/2} \qquad (\forall\, n \ge 2). \tag{4.21}$$

Remark 4.13 (Geometric Origin of the Factor-of-2 Cancellation and the $n^{1/2}$ Envelope)**.** The leading density $\frac{n}{\ln n}$ in Equation (4.21) arises from an exact geometric cancellation intrinsic to the quadratic foliation $\mathbb{N}_2$: at shell index n, the horizontal shell cardinality expands linearly as $|S_n| = (n+1)^2 - n^2 = 2n+1$, while the local prime density at scale $x \approx n^2$ dilutes logarithmically as $\frac{1}{\ln(n^2)} = \frac{1}{2\ln n}$. Their product cancels the factor of 2, yielding the expected shell prime count:

$$\mathbb{E}\big[\,|\mathcal{P}(S_n)|\,\big] \approx |S_n| \cdot \frac{1}{\ln(n^2)} = \frac{2n+1}{2\ln n} = \frac{n}{\ln n} + \frac{1}{2\ln n}.$$

Under short-interval probabilistic models of primes in intervals of length $H = 2n$ at scale $x = n^2$, the variance of $\big|\mathcal{P}(S_n)\big|$ scales as $\sigma^2(n) \sim \frac{n}{\ln n}$, corresponding to a standard deviation of $\sigma(n) \sim n^{1/2}(\ln n)^{-1/2}$. The strict envelope $n^{1/2} = \sigma(n)\sqrt{\ln n}$ in Equation (4.21) thus represents a slowly widening $\sqrt{\ln n}$-standard-deviation barrier around the holographic density $\frac{n}{\ln n}$.

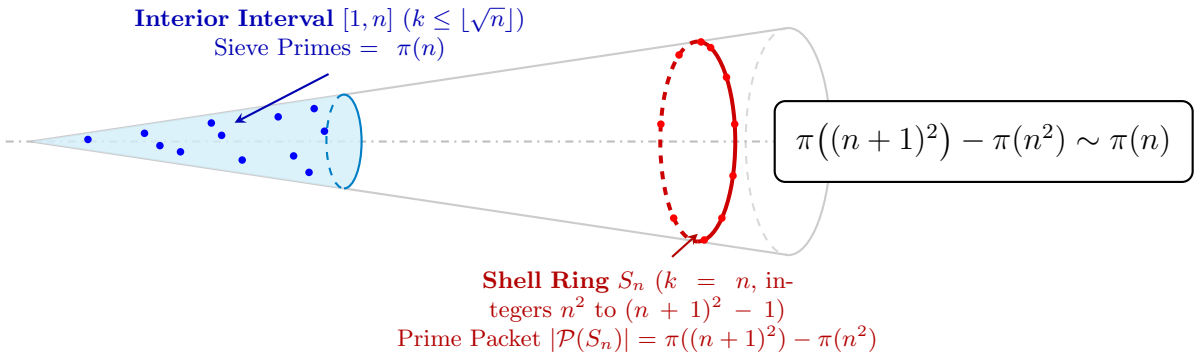


Figure 6: The Arithmetic Holographic Conjecture on the conical embedding of $\mathbb{N}_2$. The blue region contains the integers 1 to n ($k \le \lfloor\sqrt{n}\rfloor$), whose $\pi(n)$ primes sieve the distant circular shell S_n at $k = n$ (red ring), yielding $|\mathcal{P}(S_n)| = \pi((n+1)^2) - \pi(n^2) \sim \pi(n)$.

5 The Correspondence Principle: Peano Arithmetic ($m = 1$)

To prove that the m-degree foliation $\mathbb{Z}_m$ is a strict generalization of the classical one-dimensional number line, we evaluate the entire geometric, metric, and algebraic hierarchy at the degenerate boundary $m = 1$. At this limit, lateral width vanishes, the three directional frames fuse into a single trajectory, discrete holonomy and curvature collapse to zero, the geodesic transport metric reduces to the classical absolute value norm, and all foliated arithmetic operations reduce identically to classical Peano arithmetic.

5.1 Coordinate Degeneracy to the 1D Euclidean Line

For $m = 1$, the shell index k_a of any non-negative integer $a \in \mathbb{N}$ reduces to the scalar integer itself:

$$k_a = \lfloor a^{1/1} \rfloor = a. \tag{5.1}$$

The cardinality of each 1-degree shell $S_{k,1}$ is $(k+1)^1 - k^1 = 1$. Because every shell houses a single integer, the lattice possesses zero lateral width. Evaluating Equation (2.22) at $m = 1$ shows that the lateral generator vanishes identically across all directions $\lambda \in \{0, \frac{1}{2}, 1\}$:

$$g(a, \lambda) = 0, \qquad k_0(0, \lambda, 1) = 0, \qquad d_{\lambda,1}(a) = k_a - 0 = a. \tag{5.2}$$

Thus, at $m = 1$, longitudinal leaf depth $d_{\lambda,1}(a)$ and scalar magnitude a become identical, and the three leaf partitions $L_{0,1}, V_{0,1}, R_{0,1}$ collapse into the single 1D number line.

5.2 Degeneracy of Transport, Arithmetic, Division, Primality, Holonomy, and Metric

Theorem 5.1 (The Master Correspondence Theorem at $m = 1$)**.** *At the limit $m = 1$, the transport operator $\nabla_{\lambda,1}$, the binary arithmetic operations $(\oplus_1, \ominus_1, \otimes_1, \oslash_1, \mathrm{mod}_1)$, the primality classes $(\mathbb{P}_{\lambda,1}, \mathcal{D}_{\lambda,1})$, the self-shift holonomy commutator $[\widehat{T}_{\lambda_1,1}, \widehat{T}_{\lambda_2,1}]$, and the geodesic transport metric $\delta_1(x, y)$ degenerate across all directions $\lambda \in \{0, \frac{1}{2}, 1\}$ as follows:*

1. ***Single-Valued Linear Transport:*** *Equation (2.24) reduces to classical shift translation:*

$$\nabla_{\lambda,1}(a, s) = a + (1 - \lambda)\big[(a + s) - a\big] + \lambda\big[(a + s + 1) - (a + 1)\big] = a + s, \tag{5.3}$$

and on $\mathbb{Z}_1$, $\widehat{\nabla}_{\lambda,1}(z, s) = z + s$.

2. ***Commutative Addition, Subtraction, and Multiplication:*** *Equations* (3.7)–(3.8) *collapse to singletons satisfying the classical ring axioms:*

$$\begin{aligned} a \oplus_1 b &= a + b = b \oplus_1 a, \qquad a \ominus_1 b = a - b, \\ a \otimes_1 b &= \nabla_{\lambda,1}\big(a, a(b-1)\big) = a + a(b-1) = ab = b \otimes_1 a. \end{aligned} \tag{5.4}$$

3. ***Classical Euclidean Division and Modularity:*** *In Theorem 3.10, the transverse remainder vanishes ($\rho_{\lambda,1}(N,a) = 0$), while the quotient and shell remainder reduce to classical Euclidean division $N = a\lfloor N/a \rfloor + (N \bmod a)$:*

$$q(N,a) = 1 + \left\lfloor \frac{N-a}{a} \right\rfloor = \left\lfloor \frac{N}{a} \right\rfloor, \qquad \rho_k(N,a) = (N-a) \bmod a = N \bmod a. \tag{5.5}$$

4. ***Unification of Global and Local Primality:*** *Because $d_{\lambda,1}(a) = a$, Equations* (3.30) *and* (3.31) *both become $\nabla_{\lambda,1}\big(a,(x-1)a\big) = ax = p$, collapsing all directional prime sets and the co-leaf product $\odot_{\lambda,1}$ into the classical scalar primes $\mathbb{P}$ and classical multiplication:*

$$\mathbb{P}_{0,1} = \mathbb{P}_{1/2,1} = \mathbb{P}_{1,1} = \mathcal{D}_{0,1} = \mathcal{D}_{1/2,1} = \mathcal{D}_{1,1} = \mathbb{P}, \qquad x \odot_{\lambda,1} y = xy. \tag{5.6}$$

5. ***Vanishing of Discrete Holonomy and Curvature:*** *At $m = 1$, the self-shift operator $\widehat{T}_{\lambda,1}(z) = \widehat{\nabla}_{\lambda,1}(z,z) = 2z$ is independent of λ. Consequently, for all $\lambda_1, \lambda_2 \in \{0, \frac{1}{2}, 1\}$ and all $z \in \mathbb{Z}_1$:*

$$\big[\widehat{T}_{\lambda_1,1}, \widehat{T}_{\lambda_2,1}\big](z) = 4z - 4z = 0, \qquad \mathcal{R}^{(1)}_{\lambda_1,\lambda_2}(z) = 0. \tag{5.7}$$

6. ***Collapse of the Transport Geodesic Metric to Classical 1D Distance:*** *For any $x, y \in \mathbb{N}_1$ with $u = \min(x,y)$ and $v = \max(x,y)$, the lateral generator difference vanishes ($|\Delta g| = |g_v(v) - g_v(u)| = 0$), so the intermediate turning point in Equation* (2.25) *reduces to $\nabla_{\lambda^*,1}(u, |\Delta g|) = \nabla_{\lambda^*,1}(u,0) = u$. Substituting $m = 1$ and $\lfloor z^{1/1} \rfloor = z$ into Equation* (2.25) *collapses the 1-zigzag transport metric directly to the classical absolute value norm on the number line:*

$$\begin{aligned} \delta_1(x,y) &= \frac{1}{2}\left((v-u) + |\Delta g| + \Big| v - \nabla_{\lambda^*,1}(u, |\Delta g|) \Big| \right) \\ &= \frac{1}{2}\Big((v-u) + 0 + |v-u| \Big) = v - u = |x-y|. \end{aligned} \tag{5.8}$$

Proof. Each identity follows directly by substituting $m = 1$, $k_n = d_{\lambda,1}(n) = n$, and $g(n,\lambda) = 0$ into the corresponding m-degree definitions in Sections 2, 3, and 4. □

6 Discussion and Conclusion

6.1 Synthesis of the Foliated Arithmetic Framework

In this paper, we have shown that classical Peano arithmetic on the 1D line is the degenerate $m = 1$ limit of an infinite sequence of m-degree integer foliations $\mathbb{Z}_m$ ($m \geq 1$). By decoupling the shell index $k = \lfloor \sqrt[m]{|z|} \rfloor$ and local leaf depth $d_{\lambda,m}(z)$ from the scalar magnitude z, the integers acquire an intrinsic two-dimensional geometry governed by the affine transport operator $\nabla_{\lambda,m}(z,s)$ and the self-shift operator $\widehat{T}_{\lambda,m}(z) = \widehat{\nabla}_{\lambda,m}(z,z)$ across $\lambda \in \{0, \frac{1}{2}, 1\}$. Across this hierarchy:

1. Binary arithmetic operations $(\oplus_m, \ominus_m, \otimes_m, \oslash_m)$ unfold via $\nabla_{\lambda,m}$ into multi-valued triads that violate commutativity and distributivity while inducing a global Chebyshev (L^∞) geodesic metric.

2. Sequential applications of the self-shift operators $\widehat{T}_{\lambda_1}$ and $\widehat{T}_{\lambda_2}$ in $\mathbb{Z}_2$ generate non-vanishing discrete holonomy $[\widehat{T}_{\lambda_1}, \widehat{T}_{\lambda_2}](z) \neq 0$ and positive discrete curvature $\mathcal{R}_{\lambda_1,\lambda_2}(z) = 2A(|z|)|\lambda_1 - \lambda_2|$, whose normalized value $z^{-2}\mathcal{R}_{\lambda_1,\lambda_2}(z)$ converges to the constant $2|\lambda_1 - \lambda_2|$ as $|z| \to \infty$, exhibiting an asymptotic de Sitter behavior.

3. Primality bifurcates into Global λ-Foliated Primality ($\mathbb{P}_{\lambda,m}$, irreducibility under $\otimes_{\lambda,m}$) and Local Leaf-Depth Primality ($\mathcal{D}_{\lambda,m}$), which endows every structural leaf with an autonomous Fundamental Theorem of Arithmetic under $\odot_{\lambda,m}$, satisfies the exact holographic identity $|\mathcal{D}_{\lambda,2} \cap S_n| = \pi(n) + \pi(n-1)$, and underpins the Arithmetic Holographic Conjecture $\pi((n+1)^2) - \pi(n^2) \sim \pi(n)$ [15].

6.2 Structural Parallels with Theoretical Physics and Computation

For nearly a century, theoretical physics has sought to reconcile the continuous, deterministic geometry of General Relativity with the discrete, non-commutative algebra of Quantum Mechanics [16, 17]. Viewed through the lens of integer foliations, one may ask whether this tension reflects a deeper mathematical contrast between two different foliation regimes.

Classical continuum physics is built upon the arithmetic of the $m = 1$ flat line [18]: even when a macroscopic manifold is curved, its underlying real coordinates rely on single-valued, commutative scalar arithmetic where coordinate depth and magnitude coincide. By contrast, the algebraic features that characterize microscopic physics—non-commuting operators [19, 20, 21], path-dependent holonomy commutators, and multi-branched state evolution across distinct directionss—arise natively within the quadratic foliation ($m = 2$) whenever longitudinal depth is decoupled from scalar magnitude. From this perspective, the transition from a multi-branched $m = 2$ triad to a single scalar outcome in an $m = 1$ classical apparatus offers a natural mathematical analogy for dimensional projection during measurement [22, 23], while implementing multi-branch foliated operations in digital logic suggests a purely arithmetic model for parallel multi-directional computation. We leave the physical and computational interpretation of these structural parallels to specialists in those fields.

6.3 Beyond the Integers: Open Questions for Algebra and the Continuum

Throughout this work, we have constructed integer foliations by choosing the horizontal shells to be the intervals between consecutive m-th powers. Yet this polynomial family is only one natural choice among infinitely many. What if we instead partition the integers using consecutive factorials, primorials, or any other strictly increasing sequence of shell boundaries? Provided two minimal prerequisites are respected—bilateral shell symmetry (ensuring a well-defined central spine and reflection involution) and a bijective scalar indexing—the entire geometric and arithmetic architecture developed in this paper reproduces intact.

This invariance points to a deeper observation about the nature of numbers. For millennia, mathematics has operated under the implicit assumption that the counting numbers are intrinsically flat ($m = 1$), treating each integer as a dimensionless point on a one-dimensional line. Within the infinite space of symmetric foliations of the integers, however, the flat Peano line is a single degenerate boundary; in every other foliation, the integers behave natively as two-dimensional geometric objects equipped with lateral width, transverse trajectories, and internal curvature.

If the integers are the most fundamental object of mathematics, recognizing their two-dimensional geometric nature compels us to ask a broader question: *how must Abstract Algebra and the higher number systems evolve when built upon a foliated foundation?* Rather than prescribing fixed rules, we conclude by outlining four foundational questions for future investigation:

1. **How Does Abstract Algebra Evolve Beyond the Flat Line?** Classical abstract algebra—the axiomatic theory of groups, rings, fields, and modules—was constructed in the image of the flat $m = 1$ integer line, where binary operations are single-valued, commutative, and distributive. When the underlying integers are unfolded into a two-dimensional foliation where longitudinal depth decouples from scalar magnitude, single-valued operations give way to directional triads, commutativity is replaced by holonomy commutators, and unique factorization multiplies into transverse leaf-local monoids. What is the natural axiomatization of a "foliated ring" or "foliated module" when algebraic operations and geometric transport can no longer be separated?

2. **What Is the Structure of a Foliated Real Continuum?** Classical real analysis completes the flat rationals and integers into the one-dimensional continuum $\mathbb{R}$. If we instead pass to the continuum limit across an m-degree foliation, how do discrete shell indices and intra-shell offsets transition into continuous radial and angular coordinates? In such a foliated continuum, does the step-additive discrete transport operator naturally become a directional covariant derivative along the leaves, and does the discrete holonomy commutator induce a continuous curvature two-form natively on the real numbers?

3. **Do Complex Numbers Emerge Natively from Conical Foliations?** In classical mathematics, the complex plane $\mathbb{C}$ must be constructed extrinsically by adjoining the imaginary unit $i = \sqrt{-1}$ to the flat real line. Yet on the conical embedding of the quadratic foliation $\mathbb{Z}_2$, circular periodicity and reflection symmetry are already present in the geometry of each closed horizontal shell. Can complex modulus and phase be realized directly from longitudinal shell depth and intra-shell circulation, turning complex multiplication into helical transport along the foliated cone without adjoining an external imaginary axis?

4. **Can Quaternionic Non-Commutativity Originate from the Self-Shift Triad?** Hamilton's quaternions $\mathbb{H}$ require three non-commutative spatial generators alongside a scalar axis to describe three-dimensional rotation and curvature. In classical $m = 1$ arithmetic, breaking commutativity requires climbing three successive algebraic extensions ($\mathbb{Z} \to \mathbb{R} \to \mathbb{C} \to \mathbb{H}$). In a higher-degree foliation ($m \geq 2$), however, commutativity is already broken at the level of the integers themselves: every integer is governed by a one-dimensional shell depth together with three non-commuting holographic self-shift operators across the left, vertical, and right directions. Does this native $(1 + 3)$ operational structure on the integers provide a direct arithmetic precursor to the quaternionic generators and three-dimensional rotational symmetries?

Exploring these questions suggests that liberating the integers from the one-dimensional line is not an endpoint, but a starting point for rethinking the bridge between discrete arithmetic, abstract algebra, and continuous geometry.

Acknowledgments

All mathematical concepts, definitions, proofs, and theoretical results developed in this work are entirely the original creation of the author. The author acknowledges the use of a large language model (Google Gemini) for assistance with English language editing, manuscript organization, and LaTeX/TikZ typesetting. The author has verified all expressions and assumes full responsibility for the content of this paper.

References

[1] Descartes, R. (1637). *La Géométrie*. Discours de la méthode.

[2] Dedekind, R. (1888). *Was sind und was sollen die Zahlen?*. Vieweg.

[3] Peano, G. (1889). *Arithmetices principia, nova methodo exposita*. Bocca, Torino.

[4] Maudlin, T. (2014). *New Foundations for Physical Geometry: The Theory of Linear Structures*. Oxford University Press.

[5] Minkowski, H. (1910). *Geometrie der Zahlen*. Teubner.

[6] Grothendieck, A., & Dieudonné, J. (1960). *Éléments de géométrie algébrique: I. Le langage des schémas*. Publications Mathématiques de l'IHÉS, 4, 5–228.

[7] Arakelov, S. Y. (1974). *Intersection theory of divisors on an arithmetic surface*. Mathematics of the USSR-Izvestiya, 8(6), 1167–1180.

[8] Cantor, G. (1878). *Ein Beitrag zur Mannigfaltigkeitslehre*. Journal für die reine und angewandte Mathematik, 84, 242–258.

[9] Fueter, R., & Pólya, G. (1923). *Rationale Abzählung der Gitterpunkte*. Vierteljschr. Naturforsch. Ges. Zürich, 58, 280–386.

[10] Zhang, Y. (2014). *Bounded gaps between primes*. Annals of Mathematics, 179(3), 1121–1174.

[11] Maynard, J. (2015). *Small gaps between primes*. Annals of Mathematics, 181(1), 383–413.

[12] Polymath, D. H. J. (2014). *Variants of the Selberg sieve, and bounded intervals containing many primes*. Research in the Mathematical Sciences, 1(1), 12.

[13] Westzynthius, E. (1931). *Über die Verteilung der Zahlen, die zu den n ersten Primzahlen teilerfremd sind*. Commentationes Physico-Mathematicae, 5(25), 1–37.

[14] Ford, K., Green, B., Konyagin, S., Maynard, J., & Tao, T. (2018). *Long gaps between primes*. Journal of the American Mathematical Society, 31(1), 65–105.

[15] Susskind, L. (1995). *The World as a Hologram*. Journal of Mathematical Physics, 36(11), 6377–6396.

[16] Penrose, R. (2004). *The Road to Reality: A Complete Guide to the Laws of the Universe*. Jonathan Cape.

[17] Rovelli, C. (2004). *Quantum Gravity*. Cambridge University Press.

[18] Einstein, A. (1915). *Die Feldgleichungen der Gravitation*. Sitzungsberichte der Preussischen Akademie der Wissenschaften zu Berlin.

[19] Heisenberg, W. (1925). *Über quantentheoretische Umdeutung kinematischer und mechanischer Beziehungen*. Zeitschrift für Physik, 33(1), 879–893.

[20] Dirac, P. A. M. (1930). *The Principles of Quantum Mechanics*. Oxford University Press.

[21] Connes, A. (1994). *Noncommutative Geometry*. Academic Press.

[22] Von Neumann, J. (1932). *Mathematische Grundlagen der Quantenmechanik*. Springer, Berlin.

[23] Zurek, W. H. (2003). *Decoherence, einselection, and the quantum origins of the classical*. Reviews of Modern Physics, 75(3), 715.